PD IEC/TS 61244-1:2014

BSI Standards Publication

Determination of long-term radiation ageing in polymers

Part 1: Techniques for monitoring diffusion-limited oxidation

bsi.

...making excellence a habit.™

National foreword

This Published Document is the UK implementation of IEC/TS 61244-1:2014. It supersedes BS 7816-1:1995 which is withdrawn.

The UK participation in its preparation was entrusted to Technical Committee GEL/112, Evaluation and qualification of electrical insulating materials and systems.

A list of organizations represented on this committee can be obtained on request to its secretary.

This publication does not purport to include all the necessary provisions of a contract. Users are responsible for its correct application.

Published by BSI Standards Limited 2014

ISBN 978 0 580 84311 2
ICS 17.240; 29.035.20

Compliance with a British Standard cannot confer immunity from legal obligations.

This Published Document was published under the authority of the Standards Policy and Strategy Committee on 30 September 2014.

Amendments/corrigenda issued since publication

Date	Text affected

IEC TS 61244-1

Edition 2.0 2014-08

SPECIFICATION TECHNIQUE

colour inside

Determination of long-term radiation ageing in polymers – Part 1: Techniques for monitoring diffusion-limited oxidation

Détermination du vieillissement à long terme sous rayonnement dans les polymères – Partie 1: Techniques pour contrôler l'oxydation limitée par diffusion

INTERNATIONAL ELECTROTECHNICAL COMMISSION

COMMISSION ELECTROTECHNIQUE INTERNATIONALE

PRICE CODE
CODE PRIX

X

ICS 17.240; 29.035.01

ISBN 978-2-8322-1827-3

CONTENTS

FOREWORD....4
INTRODUCTION....6
1 Scope....7
2 Profiling techniques to monitor diffusion-limited oxidation....7
2.1 General....7
2.2 Infra-red profiling techniques....7
2.3 Modulus profiling....10
2.4 Density profiling....14
2.5 Miscellaneous profiling techniques....16
3 Theoretical treatments of diffusion-limited oxidation....18
4 Permeation measurements....21
5 Oxygen consumption measurements....21
6 Comparison of theory with experimental results....22
7 Oxygen overpressure technique....23
8 Summary....25
Annex A (informative) Derivation of theoretical treatment of diffusion-limited oxidation....26
A.1 General....26
A.2 Numerical simulation....29
A.3 Cylindrical and spherical geometries and simulation....30
A.4 Time dependence of the simulation....35
Bibliography....37

Figure 1 – Relative oxidation as determined from the carbonyl absorbance versus depth away from air-exposed surface of polyolefin material after ageing for 6 days at 100 °C (from [18])....8
Figure 2 – Depth distribution of carbonyl groups in irradiated (0,69 Gy/s) multilayer samples composed of 4, 18, 27 and 44 films of 22 μm thickness....9
Figure 3 – Micro-FTIR spectrophotometric determination of photoproduct and of residual double-bond profiles in a SBR film photooxidized for 100 h....10
Figure 4 – Schematic diagram of modulus profiling apparatus....11
Figure 5 – Modulus profiles of 1,68 mm thick commercial fluoro elastomer samples after air ageing at 5,49 kGy/h and 70 °C to the indicated radiation doses (from [15])....12
Figure 6 – Modulus profiles of 1,68 mm thick commercial fluoro elastomer samples after air ageing at 0,90 kGy/h and 70 °C to the indicated radiation doses (from [15])....12
Figure 7 – Modulus profiles of 1,68 mm thick commercial fluoro elastomer samples after air ageing at 0,14 kGy/h and 70 °C to the indicated radiation doses (from [15])....13
Figure 8 – Modulus profiles of 1,9 mm thick chloroprene rubber samples following elevated temperature exposures in the presence of air at 150 °C, left plot, and 100 °C, right plot (from [10])....13
Figure 9 – Experimental density profiles (crosses) for 0,302 cm (left) and 0,18 cm (right) thick EPDM sheets after ageing at 6,65 kGy/h and 70 °C in airX-ray microanalysis....14
Figure 10 – Effect of total radiation dose on XMA profile for 2 mm thick EPDM sheet irradiated at 1 kGy/h in air (from [24])....15

Figure 11 – XMA profiles of 1 mm thick EPDM sheets after thermal ageingin air (from [24])16

Figure 12 – NMR self-diffusion coefficients versus distance away from sample surface for low-density polyethylene samples after gamma-irradiation in air or vacuum at 0,6 Gy/sec for the indicated total doses (from [26])....17

Figure 13 – Chemiluminescence profile for a polypropylene material after gamma irradiation in air to 0,05 MGy at 2 kGy/h (data from [30])....17

Figure 14 – Theoretical oxidation profiles for various values of α (indicated in the figure) with β = 0,1....19

Figure 15 – Identical to Figure 14, except that β = 10 20

Figure 16 – Identical to Figure 14, except that β = 1 000....20

Figure 17 – Plot of $\alpha_c/(\beta + 1)$ versus β, where α_c denotes the value of integrated oxidation corresponding to 90 % (from [7, 23])....21

Figure 18 – Apparatus used for irradiation under pressurized oxygen conditions 24

Figure 19 – Tensile elongation (left) and tensile strength (right) data for an EPR material aged at the indicated high and low dose-rates in air and at high dose rate in the pressurized oxygen apparatus of Figure 18....25

Figure A.1 – Simplified kinetic scheme used to represent the oxidation of polymers (from [44, 45])....26

Figure A.2 – Typical example of normalized concentration of oxygen for cylindrical shape for β=0,01 from [46]....31

Figure A.3 – Typical example of relative oxygen consumption for cylindrical shape for β=0,01 from [46]....31

Figure A.4 – Typical example of normalized concentration of oxygen for cylindrical shape for β=100 from [46]....32

Figure A.5 – Typical example of relative oxygen consumption for cylindrical shape for β=100 [46]....32

Figure A.6 – Typical example of normalized concentration of oxygen for spherical shape for β=0,01 from [46]....33

Figure A.7 – Typical example of relative oxygen consumption for spherical shape for β=0,01 from [46]....33

Figure A.8 – Typical example of normalized concentration of oxygen for spherical shape for β=100 from [46]....34

Figure A.9 – Typical example of relative oxygen consumption for spherical shape for β=100 [46]....34

Figure A.10 – Typical example of time-dependent normalized concentration of oxygen at the centre from for the case of β=1 [46]....35

Figure A.11 – Typical example of time-dependent normalized concentration of oxygen at the centre from for the case of α=50 [46]....36

INTERNATIONAL ELECTROTECHNICAL COMMISSION

_____

DETERMINATION OF LONG-TERM RADIATION AGEING IN POLYMERS –

Part 1: Techniques for monitoring diffusion-limited oxidation

FOREWORD

1) The International Electrotechnical Commission (IEC) is a worldwide organization for standardization comprising all national electrotechnical committees (IEC National Committees). The object of IEC is to promote international co-operation on all questions concerning standardization in the electrical and electronic fields. To this end and in addition to other activities, IEC publishes International Standards, Technical Specifications, Technical Reports, Publicly Available Specifications (PAS) and Guides (hereafter referred to as "IEC Publication(s)"). Their preparation is entrusted to technical committees; any IEC National Committee interested in the subject dealt with may participate in this preparatory work. International, governmental and non-governmental organizations liaising with the IEC also participate in this preparation. IEC collaborates closely with the International Organization for Standardization (ISO) in accordance with conditions determined by agreement between the two organizations.
2) The formal decisions or agreements of IEC on technical matters express, as nearly as possible, an international consensus of opinion on the relevant subjects since each technical committee has representation from all interested IEC National Committees.
3) IEC Publications have the form of recommendations for international use and are accepted by IEC National Committees in that sense. While all reasonable efforts are made to ensure that the technical content of IEC Publications is accurate, IEC cannot be held responsible for the way in which they are used or for any misinterpretation by any end user.
4) In order to promote international uniformity, IEC National Committees undertake to apply IEC Publications transparently to the maximum extent possible in their national and regional publications. Any divergence between any IEC Publication and the corresponding national or regional publication shall be clearly indicated in the latter.
5) IEC itself does not provide any attestation of conformity. Independent certification bodies provide conformity assessment services and, in some areas, access to IEC marks of conformity. IEC is not responsible for any services carried out by independent certification bodies.
6) All users should ensure that they have the latest edition of this publication.
7) No liability shall attach to IEC or its directors, employees, servants or agents including individual experts and members of its technical committees and IEC National Committees for any personal injury, property damage or other damage of any nature whatsoever, whether direct or indirect, or for costs (including legal fees) and expenses arising out of the publication, use of, or reliance upon, this IEC Publication or any other IEC Publications.
8) Attention is drawn to the Normative references cited in this publication. Use of the referenced publications is indispensable for the correct application of this publication.
9) Attention is drawn to the possibility that some of the elements of this IEC Publication may be the subject of patent rights. IEC shall not be held responsible for identifying any or all such patent rights.

The main task of IEC technical committees is to prepare International Standards. In exceptional circumstances, a technical committee may propose the publication of a technical specification when

- the required support cannot be obtained for the publication of an International Standard, despite repeated efforts, or
- the subject is still under technical development or where, for any other reason, there is the future but no immediate possibility of an agreement on an International Standard.

Technical specifications are subject to review within three years of publication to decide whether they can be transformed into International Standards.

IEC TS 61244-1, which is a technical specification, has been prepared by IEC technical committee 112: Evaluation and qualification of electrical insulating materials and systems.

This second edition cancels and replaces the first edition published in 1993 and constitutes a technical revision.

This edition includes the following significant technical changes with respect to the previous edition:

a) numerical simulation of DLO is much improved;

b) geometry of samples has been expanded from only the case of the infinite plane to the cylindrical and the spherical cases.

The text of this specification is based on the following documents:

Enquiry draft	Report on voting
112/287/DTS	112/304/RVC

Full information on the voting for the approval of this technical specification can be found in the report on voting indicated in the above table.

This publication has been drafted in accordance with the ISO/IEC Directives, Part 2.

A list of all parts in the IEC 61244 series, published under the general title *Determination of long-term ageing in polymers*, can be found on the IEC website.

The committee has decided that the contents of this publication will remain unchanged until the stability date indicated on the IEC web site under "http://webstore.iec.ch" in the data related to the specific publication. At this date, the publication will be

- transformed into an International standard,
- reconfirmed,
- withdrawn,
- replaced by a revised edition, or
- amended.

IMPORTANT – The 'colour inside' logo on the cover page of this publication indicates that it contains colours which are considered to be useful for the correct understanding of its contents. Users should therefore print this document using a colour printer.

INTRODUCTION

It is usually necessary to estimate the anticipated lifetime of a polymeric material in various usage environments. For extended lifetimes (years), this often requires the application of accelerated ageing techniques which typically involve the modelling of results obtained at higher-than-ambient environmental stress levels. For many practical applications, air is present during environmental exposures – this usually implies that important oxidation effects underlie the degradation of the material. Unfortunately, exposure of polymers to air during ageing often results in inhomogeneously oxidized samples, a complication which affects attempts both to understand the oxidation process and to extrapolate accelerated exposures to long-term conditions.

The most important inhomogeneous oxidation complication involves diffusion-limited oxidation. The significance of this complication in various environments, including thermal [1] [1] radiation [2 to 4] and ultraviolet [5] has been recognized for many years. Diffusion-limited oxidation can occur whenever the rate of oxygen consumption in a material is greater than the rate at which oxygen can be resupplied to the interior of the material by diffusion processes from the surrounding air atmosphere. Such instances result in a smooth drop in the oxygen concentration from its equilibrium sorption value at the sample surfaces to a diminished or non-existent value in the sample interior. This will usually lead to a heterogeneity in the oxidation across the material, with equilibrium oxidation (e.g. corresponding to air-saturated conditions) occurring at the sample surfaces, and reduced or little oxidation in the interior.

The importance of the effect will clearly depend upon the material geometry, coupled with the oxygen consumption rate, the oxygen permeability coefficient and the oxygen partial pressure surrounding the sample [5 to 8]. Since the oxygen consumption rate will typically depend upon the environmental stress level (e.g. temperature, radiation dose rate) and both the consumption rate and the permeability coefficient may change as the material degrades [9, 10], the importance of diffusion-limited oxidation will also vary with stress level and degradation. This often implies that the percentage of the sample which is oxidized under accelerated (higher-level) environmental conditions is substantially lower than the percentage oxidized under lower-level application conditions [5 to 7, 10 to 16]. Thus, as has been clear for many years, in order to confidently extrapolate shorter-term accelerated simulations to long-term, air-ageing conditions, a critical requirement is the ability to monitor and quantitatively understand diffusion-limited oxidation effects.

Since a great deal of progress has recently been made in this area, this goal is now realistic. The purpose of this specification is to review this area. Clause 2 describes experimental profiling methods which can be used to monitor diffusion-limited oxidation. Theoretical descriptions of the phenomenon are briefly given in Clause 3. Since the shapes of the theoretical profiles depend upon the oxygen permeability coefficient and the oxygen consumption rate, these quantities are measured or estimated in order to quantitatively validate the theories. Many experimental methods have been developed for measuring permeability coefficients and a large number of experimental values are available in the literature. Clause 4 introduces some of the important literature. Experimental methods for estimating oxygen consumption rates is briefly reviewed in Clause 5. Experimental data supporting the theoretical treatments is presented in Clause 6. Once confidence in the theoretical treatments exists, the theories can be used either to choose experimental ageing conditions so that diffusion effects are unimportant, or to predict the importance of such effects. If it is impossible to eliminate diffusion effects under air ageing conditions, increasing the oxygen pressure surrounding the sample during ageing may, in certain instances, be used to achieve the desired goal, as outlined in Clause 7 on the oxygen overpressure technique.

Part 2 is published as a separate specification and describes procedures for predicting radiation ageing at low dose rates.

---

1 Figures in square brackets refer to the Bibliography.

DETERMINATION OF LONG-TERM RADIATION AGEING IN POLYMERS –

Part 1: Techniques for monitoring diffusion-limited oxidation

1 Scope

This part of IEC TS 61244, which is a technical specification, reviews experimental techniques to quantitatively monitor the effects when oxygen is present during ageing of polymers in various environments including temperature, radiation or ultraviolet.

Inhomogenous ageing effects caused by diffusion-limited oxidation are often encountered and provide theoretical equations to estimate their importance. These effects make it difficult to understand the ageing process and to extrapolate accelerated exposure to long-term conditions.

It is widely known that mechanical properties degrade prior to electrical properties.These changes are consequences of chemical changes such as oxidation. In this technical specification, only mechanical or chemical monitoring techniques are of interest.

This technical specification does not deal with electrical monitoring techniques.

2 Profiling techniques to monitor diffusion-limited oxidation

2.1 General

The presence of diffusion-limited oxidation effects implies that various properties related to the amount of oxidation will depend upon spatial location in the material. Thus, any technique which can profile (map) these spatial variations will allow diffusion-limited oxidation to be monitored. Since polymer geometries utilize cross-sections down to a few millimetres or less, and since diffusion-limited oxidation effects are operative over such small dimensions, a useful profiling technique has to have a resolution of at least 100 μm. An additional problem related to sensitivity is the observation that severe polymer degradation typically corresponds to less than 1 % of the polymer being oxidized. Thus, a useful profiling technique shall have reasonable resolution, good sensitivity to the small chemical changes which occur, wide applicability and relative ease of operation and analysis. A number of particularly useful techniques are briefly described in this clause.

2.2 Infra-red profiling techniques

Because of the ability to provide detailed chemical information on thin film samples, infra-red spectroscopy has been used to monitor diffusion-limited oxidation effects for more than 25 years [17]. Any oxidation-sensitive infra-red peak that can be monitored, either as a function of sample thickness, or as a function of sequentially microtomed slices, will yield information on oxidation heterogeneities. Many of the studies to date have concentrated on the carbonyl region (approximately 1 720 cm^{-1}) of polyolefin materials, such as polyethylene and polypropylene, since infra-red peaks in this region are characterized by high extinction coefficients (high sensitivities) and are usually absent from these materials when unaged. Since the carbonyl region typically represents a superposition of a number of oxidation products (e.g. ketones, aldehydes, esters, acids) of differing extinction coefficients at slightly different wavelengths, simplifying assumptions are often needed to extract semi-quantitative information. In most cases, either the maximum height of the hybrid carbonyl peak or its area is chosen. It should be noted that additives present in commercially formulated materials (e.g. antioxidants, fire retardants) often absorb in the carbonyl region, thereby complicating attempts to use FTIR spectrometry for these materials.

An example of an infra-red profile obtained after microtoming slices off an aged material is shown in Figure 1 [18]. A polyolefin material was aged in air for 6 days at 100 °C and the relative oxidation (the absorbance of the carbonyl peak) is plotted versus the depth away from the air-exposed sample surface. The oxidation drops with depth with an approximate exponential dependence; similarly shaped profiles are often observed for heat-aged materials [10, 13, 14].

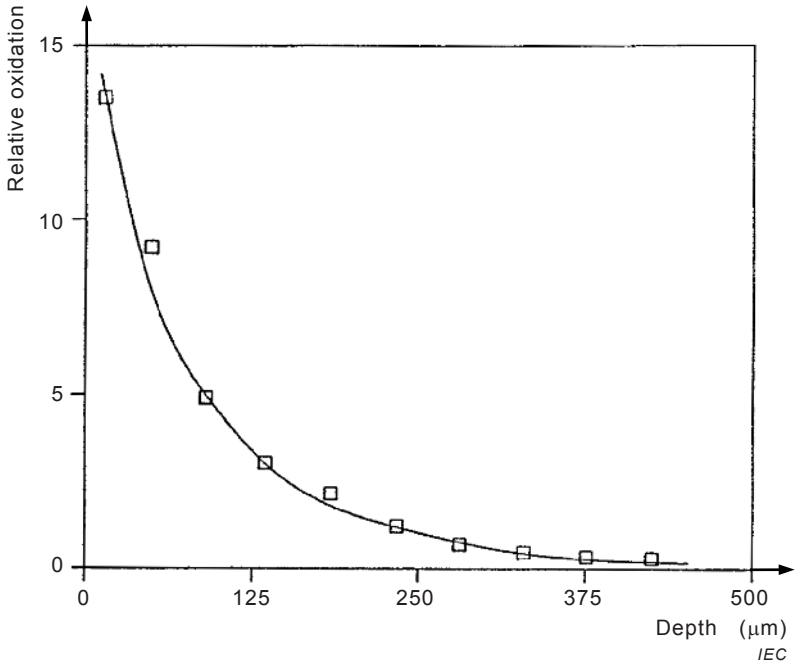

Figure 1 – Relative oxidation as determined from the carbonyl absorbance versus depth away from air-exposed surface of polyolefin material after ageing for 6 days at 100 °C (from [18])

A second infra-red approach is to create multilayer samples by packing thin films together under mechanical pressure. After ageing, the individual films are separated then individually analysed. Carbonyl profiles obtained in this fashion for gamma-radiation ageing in air of an unstabilized low-density polyethylene material are shown in Figure 2 [19]. The profiles are symmetrical, since both surfaces of the multilayer samples were exposed to air. For these samples, the profiles show a fairly abrupt transition between completely oxidized and unoxidized regions, quite different behaviour from the "exponential" shape observed in Figure 1.

Another interesting advance is the use of micro FTIR spectroscopy as a profiling method. Jouan and co-workers [20, 21] pioneered this approach and have used it in photo-oxidation studies to profile the carbonyl peak of a PVC material [20], and product profiles for styrene-butadiene (SBR) and nitrile rubbers [21]. Figure 3 shows product profiles for an SBR film photo-oxidized for 100 h and surrounded on both sides by air [21]. In this case, the drop-off in oxidation away from the surface is similar in shape to the result shown in Figure 1.

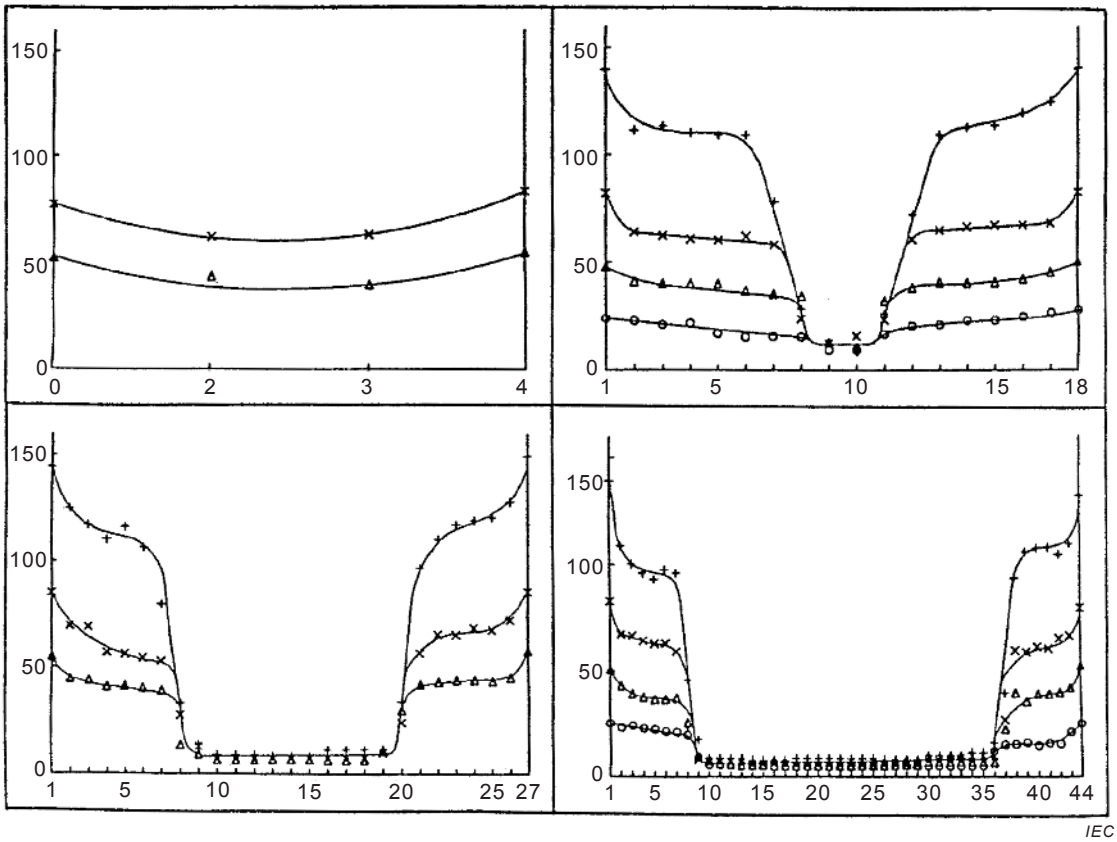

Key

○ 0,14

Δ 0,30

× 0,45

\+ 0,60 MGy (from [19])

Figure 2 – Depth distribution of carbonyl groups in irradiated (0,69 Gy/s) multilayer samples composed of 4, 18, 27 and 44 films of 22 μm thickness

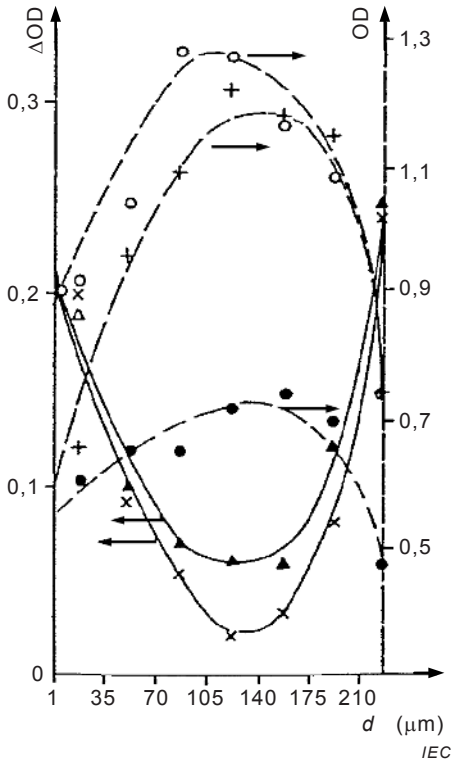

Key

▲	carbonyl at 1 717 cm^{-1}	+	1,4-*trans* at 962 cm^{-1}
×	hydroxyl at 3 440 cm^{-1}	●	1,2 at 910 cm^{-1}
○	1,4-*cis* at 700 cm^{-1}	*d*	represents the width of the slice (from [21])

Figure 3 – Micro-FTIR spectrophotometric determination of photoproduct and of residual double-bond profiles in a SBR film photooxidized for 100 h

2.3 Modulus profiling

The modulus profiling technique [14, 15] allows one to obtain rapidly and accurately more than 20 quantitative tensile compliance (*D*) measurements per millimeter of sample cross-section (1/*D* is closely related to the tensile modulus of the material). This technique is especially useful for elastomers, since the modulus of such materials is very sensitive to scission and cross-linking events and therefore to processing and ageing.

The instrument, which is based on modifications of a thermomechanical analyser, is shown schematically in Figure 4. The apparatus measures the indentation of a tiny, paraboloidally-tipped indentor into the sample. A tiny vice (shown in the figure), is used to hold the cross-sectioned samples. After the vice assembly is metallographically polished, indentation measurements under a chosen load are made at selected locations across the cross-sectioned surface. An optical microscope and an X-Y-Z linear positioner are used to quantify the measurement locations. For samples of rectangular cross-section, three samples are held in the vice in a sandwich arrangement with the profiling done across the middle sample. This avoids edge artefacts caused by the high-modulus aluminum plates used as part of the vice. The accuracy (within better than ±10 % of conventional modulus measurements), reproducibility (typically better than ±5 %) and linearity (with load) of the apparatus have been demonstrated on a variety of elastomeric materials [14].

Figures 5, 6 and 7 show modulus profile results for 1,68 mm thick sheets of a commercial fluoro elastomer rubber, which were gamma-radiation aged in air at 70 °C at three different dose rates. The data are plotted on a normalized thickness basis in which the ordinate, *P*, represents the percentage of the distance from one air-exposed surface of the sample to the opposite air-exposed surface. These profiles have shapes that appear to be intermediate between the "exponential" or "U-shaped" profiles shown in Figures 1 and 3 and the "step-

shaped" profiles shown in Figure 2. For unaged commercial fuoro elastomer, the modulus is independent of cross-sectional position and equal to 5,4 MPa; this result is denoted by the horizontal line labelled "unaged". At the highest radiation dose rate of 5,49 kGy/h (Figure 5), spectacular heterogeneity, caused by diffusion-limited oxidation, develops with ageing. Oxidative scission occurs near the air-exposed sample surfaces, leading to rapid decreases in modulus. Ageing occurs under essentially anaerobic (inert) conditions in the sample interior, yielding a cross-link-dominated increase in modulus. Since the heterogeneity can be observed after less than 0,04 MGy, which corresponds to relatively moderate changes (10 % to 20 %) in ultimate tensile properties [6, 7, 11], modulus profiling can clearly be sensitive to the earlier stages of ageing. Figure 6 gives results at a six times lower dose rate of 0,9 kGy/h, where diffusion-limited oxidation effects are reduced but still evident. Finally, at 0,14 kGy/h (Figure 7), oxidation has been slowed down sufficiently to assure homogeneous oxidation throughout the sample. When high dose-rate is adopted for radiation ageing, which is typically in accelerated ageing conditions, cross-linking is macroscopically dominant; on the other hand, in the case of low dose-rate and long-term radiation ageing, scission is dominant. Such results clearly underscore the danger that occurs whenever important diffusion-limited oxidation effects exist for accelerated environments, if the accelerated results are used to make predictions under long-term, low-level environments.

Modulus profiling results [10] for 1,9 mm thick chloroprene rubber samples after ageing in an air-circulating oven at 150 °C and 100 °C are shown in Figure 8. Significant and complicated diffusion-limited oxidation effects are evident. At the higher temperature of 150 °C (left plot), diffusion effects exist at the earliest stages of ageing. At the lower temperature of 100 °C (right plot), diffusion effects appear to be less important. In fact, at the early stages of ageing, the oxidation appears to be essentially homogeneous. In the later stages of ageing, however, important diffusion effects become apparent. This phenomenon, of increasingly important diffusion-limited effects with ageing time, is common for elastomers which are thermally aged in air. It is often caused by substantial decreases in oxygen permeation rate which occur as the polymer hardens (modulus increases) with progressive ageing. Other factors contribute [10], for example, the rate of oxygen consumption may increase with ageing time. Sorting out these complicated diffusion-limited effects is clearly necessary if results from accelerated temperature exposures are used to make long-term predictions at much lower temperatures.

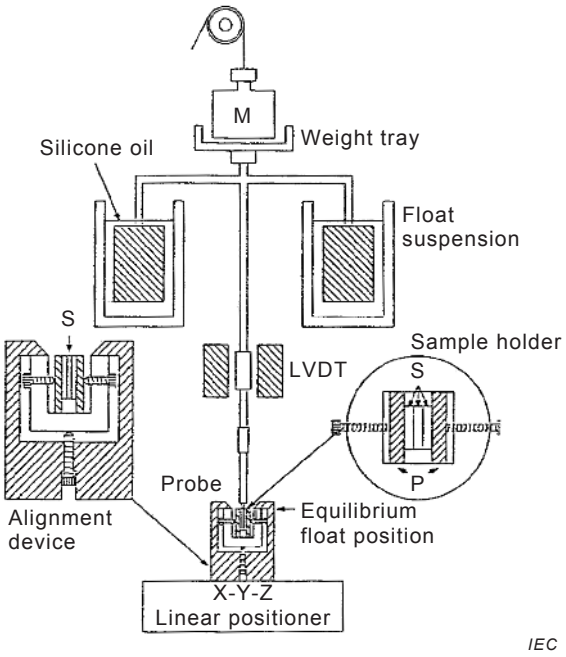

NOTE The detailed top view of the sample-holder shows three samples labelled with an S held between metal plates P. The detail to the left shows a side view of the sample-holder held in the alignment device (from [14, 15]).

Figure 4 – Schematic diagram of modulus profiling apparatus

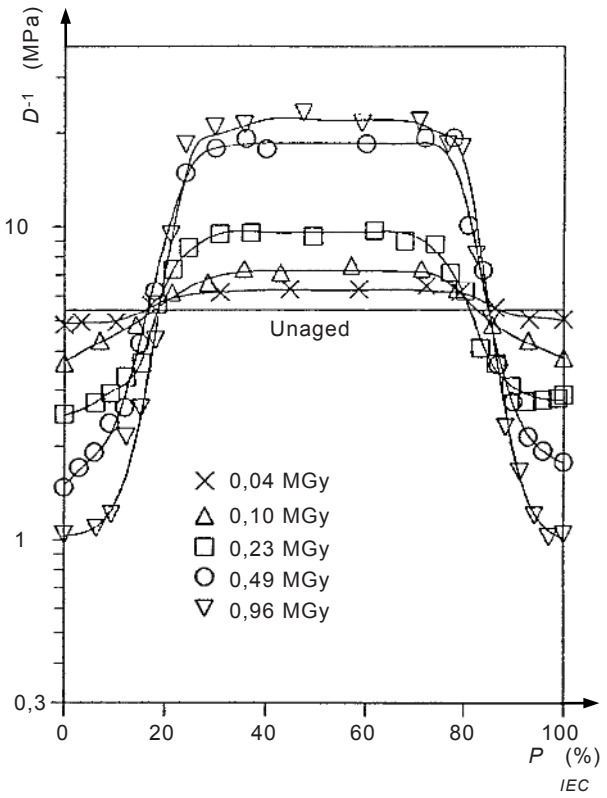

Figure 5 – Modulus profiles of 1,68 mm thick commercial fluoro elastomer samples after air ageing at 5,49 kGy/h and 70 °C to the indicated radiation doses (from [15])

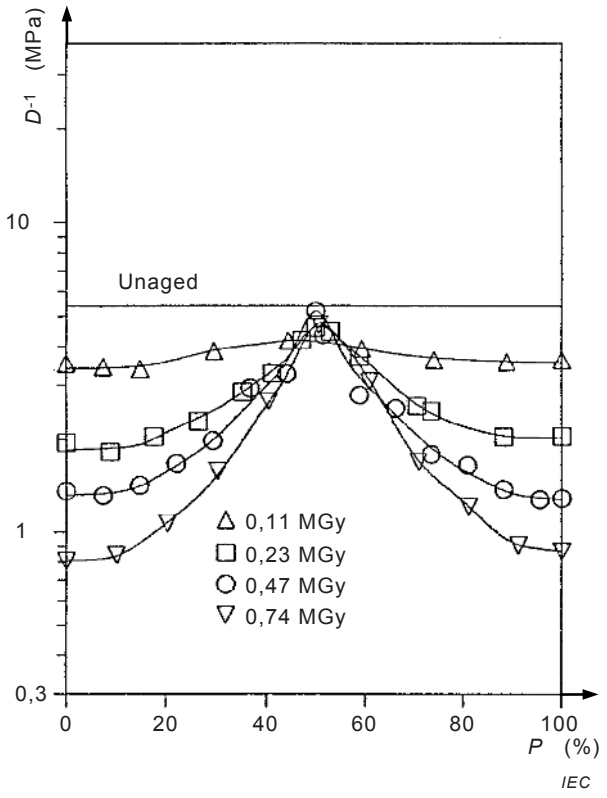

Figure 6 – Modulus profiles of 1,68 mm thick commercial fluoro elastomer samples after air ageing at 0,90 kGy/h and 70 °C to the indicated radiation doses (from [15])

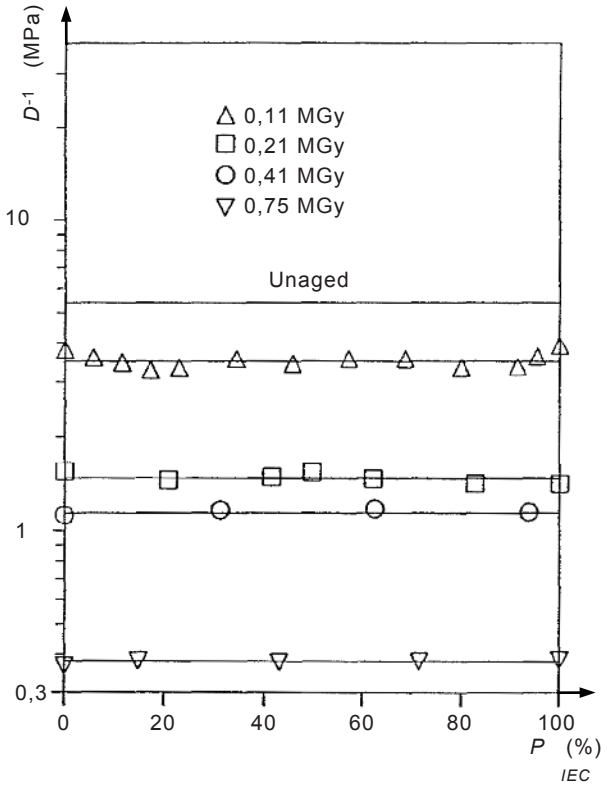

Figure 7 – Modulus profiles of 1,68 mm thick commercial fluoro elastomer samples after air ageing at 0,14 kGy/h and 70 °C to the indicated radiation doses (from [15])

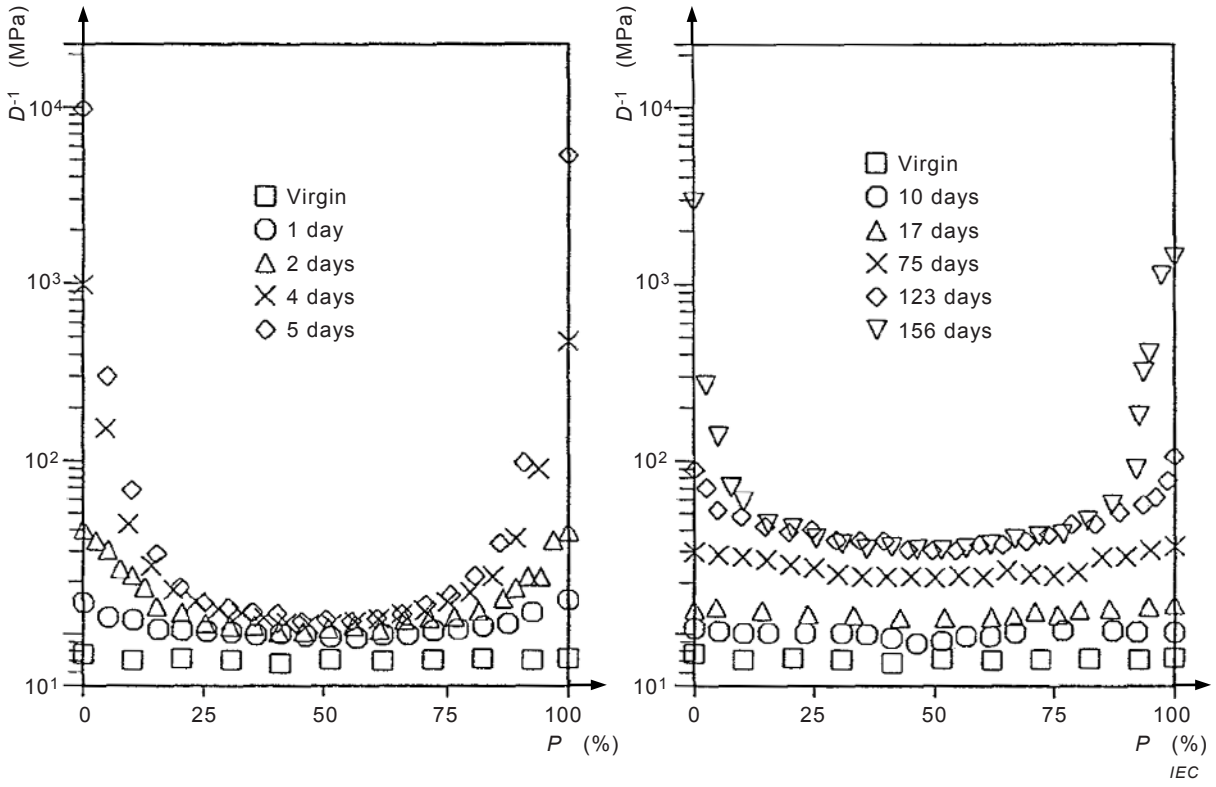

Figure 8 – Modulus profiles of 1,9 mm thick chloroprene rubber samples following elevated temperature exposures in the presence of air at 150 °C, left plot, and 100 °C, right plot (from [10])

2.4 Density profiling

The density profiling technique [13] is based on the use of a density gradient column to obtain the density of successive thin slices cut across a sample. It depends on the fact that oxidation reactions often lead to substantial and easily measurable increases in polymer density. Although a number of methods are available for measuring density, only the density gradient column can yield accurate results on the extremely small samples necessary for achieving the required spatial resolution. To use the density profiling approach, one has to find liquids for the column that are not significantly absorbed by the polymer, since swelling of the material will complicate the interpretation of the data. Since absorption of water by most polyolefins is small, density profiling has been successfully applied to these materials using aqueous salt solutions. Some example density profiling data are plotted in Figure 9 for two thicknesses of a commercially formulated EPDM rubber material after radiation ageing in air to 0,32 MGy at 6,65 kGy/h and 70 °C [22]. Since the amount of oxidation is approximately linearly related to the density increase, density changes are plotted as crosses versus cross-sectional position. The vertical span of each cross represents the estimated experimental uncertainty of the measurement, whereas the horizontal span denotes the position and thickness of each slice. The shape of these profiles again lies in the regime that is intermediate between "U-shaped" and "step-shaped". As expected, diffusion-limited oxidation effects become less important as the sample thickness is reduced.

Since density profiling is a much more difficult and time-consuming technique than modulus profiling, the latter technique is generally preferred where applicable, especially for elastomers. However, under certain ageing conditions, elastomers may degrade with an approximate balance between scission and cross-linking events, implying little sensitivity of modulus to ageing. In such instances, density profiling may prove helpful.

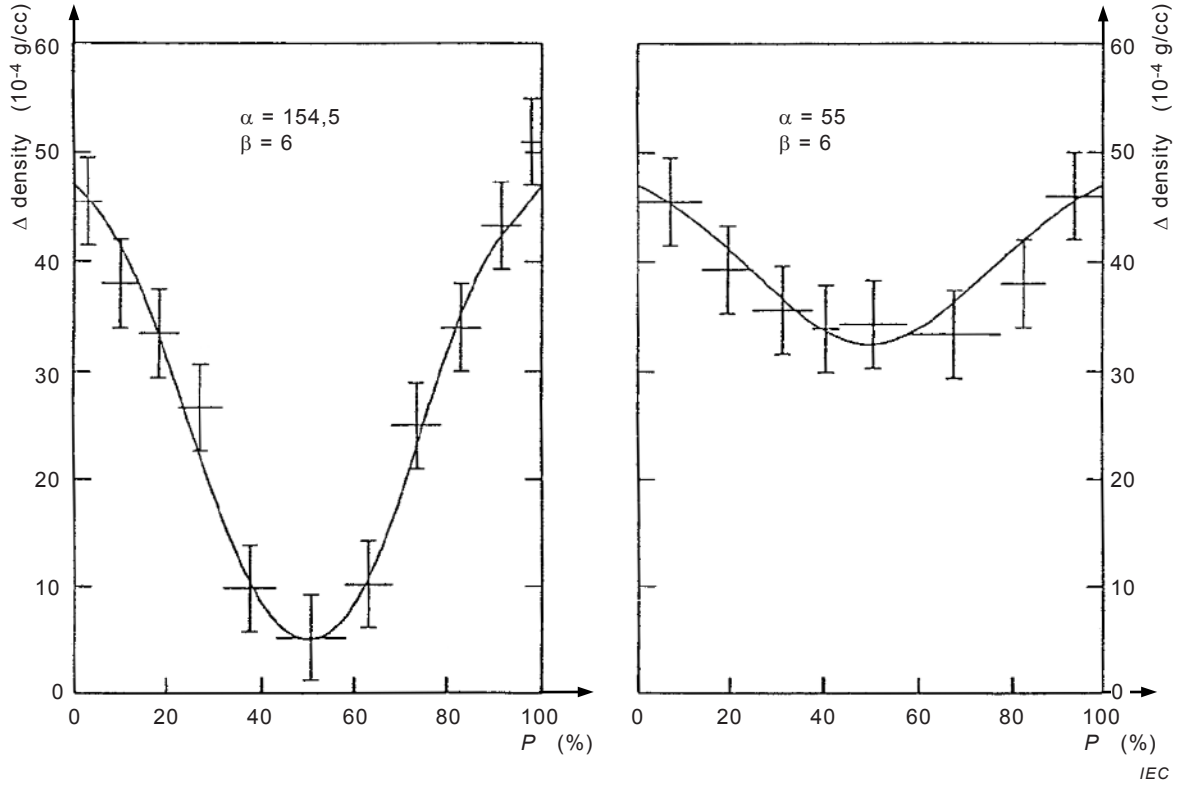

NOTE The curves give theoretical fits to the experimental results (from [22, 23]).

Figure 9 – Experimental density profiles (crosses) for 0,302 cm (left) and 0,18 cm (right) thick EPDM sheets after ageing at 6,65 kGy/h and 70 °C in airX-ray microanalysis

Another developed technique for monitoring diffusion-limited oxidation effects involves the use of X-ray microanalysis (XMA) [24]. During oxidation, common products which result on

the polymer chain are carboxyl containing groups and peroxide groups. After ageing, a cross-sectional slice of the material is exposed and dipped in a 0,1 N KOH- isopropanol solution in order to convert these groups to potassium-containing species. After conversion, the profile of potassium will therefore represent the oxidation profile for these two oxidation species. The potassium distribution is measured using an electron probe X-ray microanalyser [24].

Figure 10 shows some representative results for an EPDM material which was radiation aged in air at 1 kGy/h and room temperature. The results indicate that the thickness of the oxidized region is reasonably constant up to doses of at least 330 kGy, implying that the oxygen consumption rate and the oxygen permeability coefficients are reasonably constant up to this dose. Figure 11 shows XMA profiles for this same material after various thermal ageing exposures. It is interesting to note from the 70 °C results, that homogeneous oxidation occurs for ageing times up to 4 000 h, but that heterogeneous behaviour becomes significant at longer times. This clearly indicates that the permeability and/or the consumption rate change significantly with ageing time. It is also interesting to note the very different profile shapes observed for the two different ageing environments (radiation versus thermal). In fact, the general shapes observed with all of the profiling techniques for thermal ageing exposures (see Figures 1, 8 and 11) and for radiation exposures (see Figures 2, 5, 6, 9 and 10) are similar.

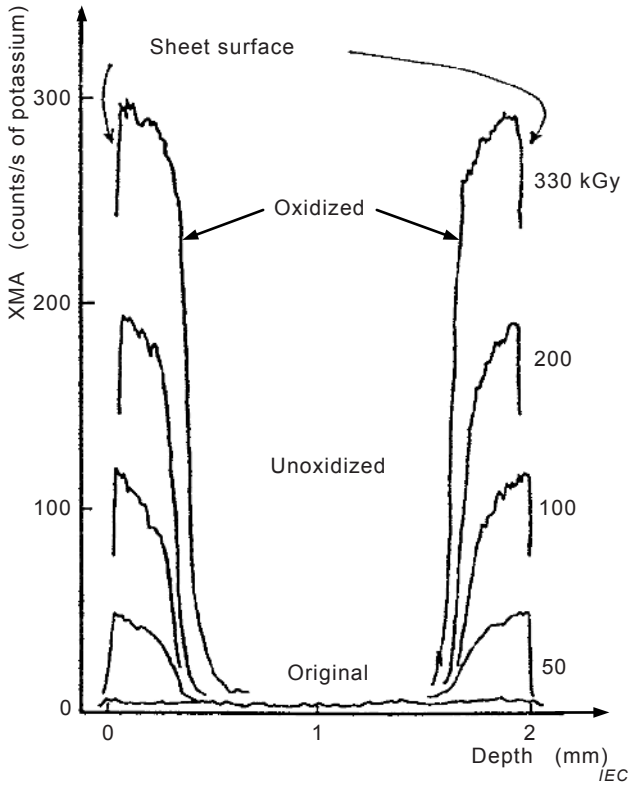

Figure 10 – Effect of total radiation dose on XMA profile for 2 mm thick EPDM sheet irradiated at 1 kGy/h in air (from [24])

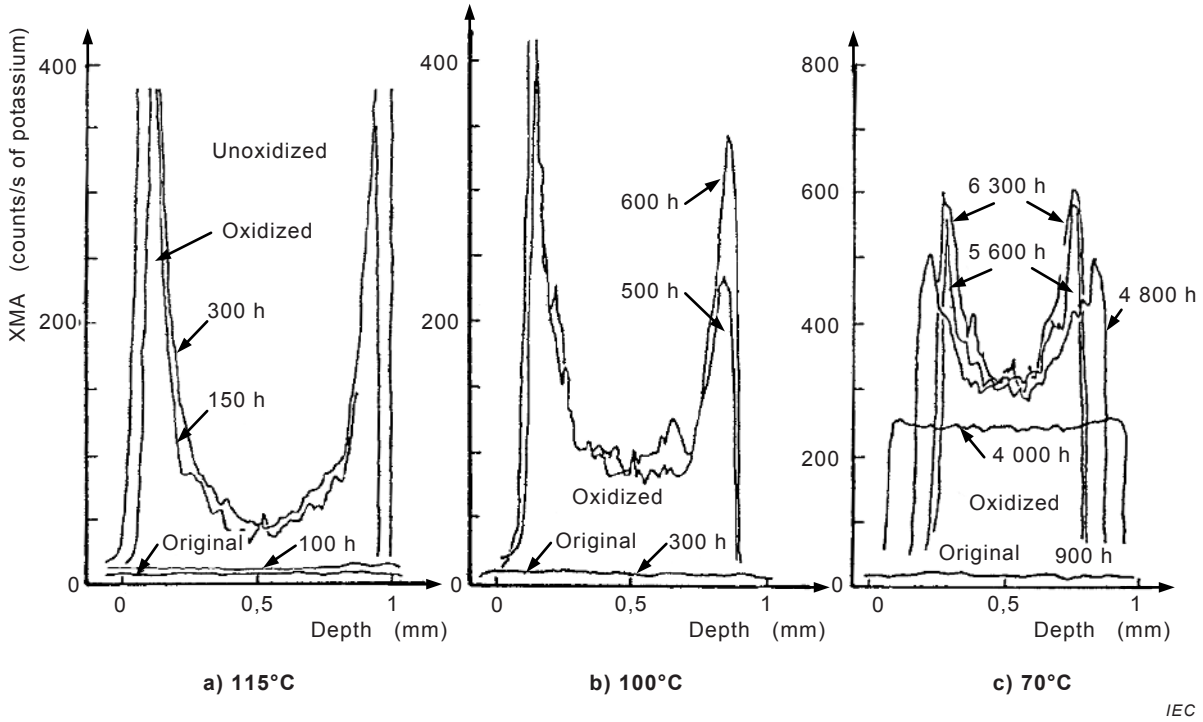

Figure 11 – XMA profiles of 1 mm thick EPDM sheets after thermal ageing in air (from [24])

2.5 Miscellaneous profiling techniques

A number of other techniques have shown some promise as profiling tools. For soluble materials, Bowmer and co-workers [25] have used gel permeation chromatography as a method to derive profiles for scission and cross-linking. Another technique sensitive to cross-linking involves the use of nuclear magnetic resonance pulsed field gradient measurements of a material's self-diffusion constant to profile diffusion-limited oxidation effects [26]. Figure 12 shows some results for low-density polyethylene samples radiation aged in air and vacuum. Wilski and co-workers [27, 28] pioneered the use of viscosity profiles to show the importance of diffusion effects for gamma-irradiated polyethylene, polypropylene and PVC. Kuriyama *et al*. [29] obtained gel fraction profiles versus dose rate for gamma-irradiated polyethylene. Chemiluminescence has been successfully applied to gamma-irradiated polypropylene samples by Yoshii *et al*. [30]. Figure 13 shows some of their results. A review has been written on experimental methods for monitoring heterogeneous oxidation and covers in more detail many of the above profiling techniques as well as a number of other potentially useful experimental approaches [6].

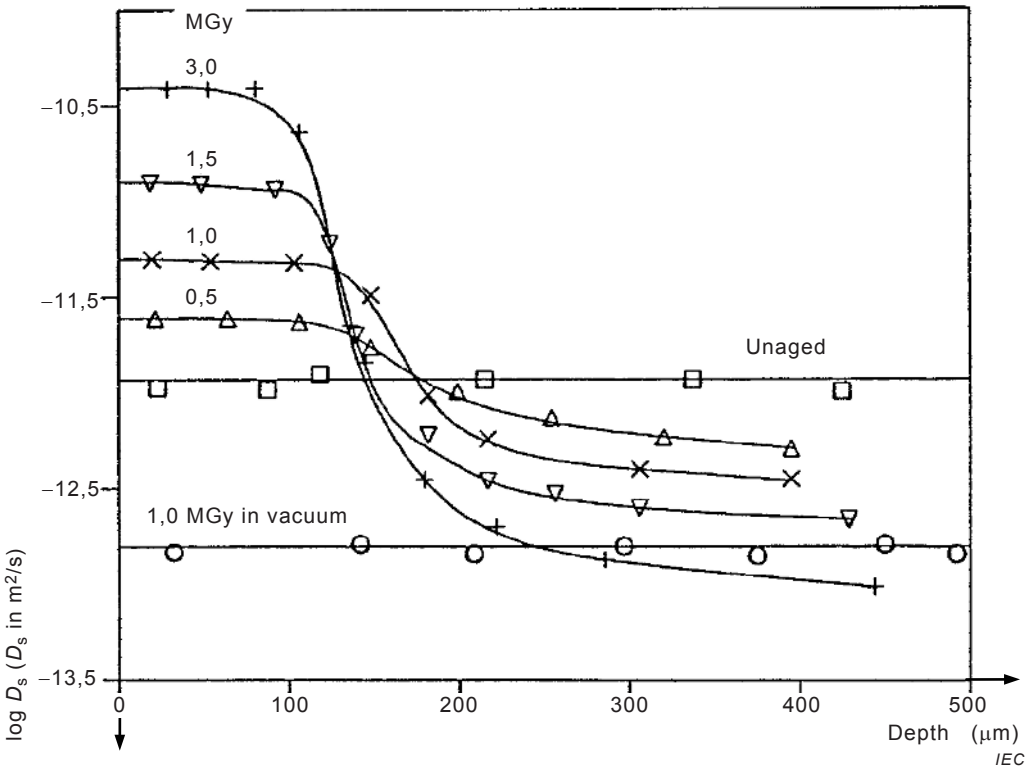

Figure 12 – NMR self-diffusion coefficients versus distance away from sample surface for low-density polyethylene samples after gamma-irradiation in air or vacuum at 0,6 Gy/sec for the indicated total doses (from [26])

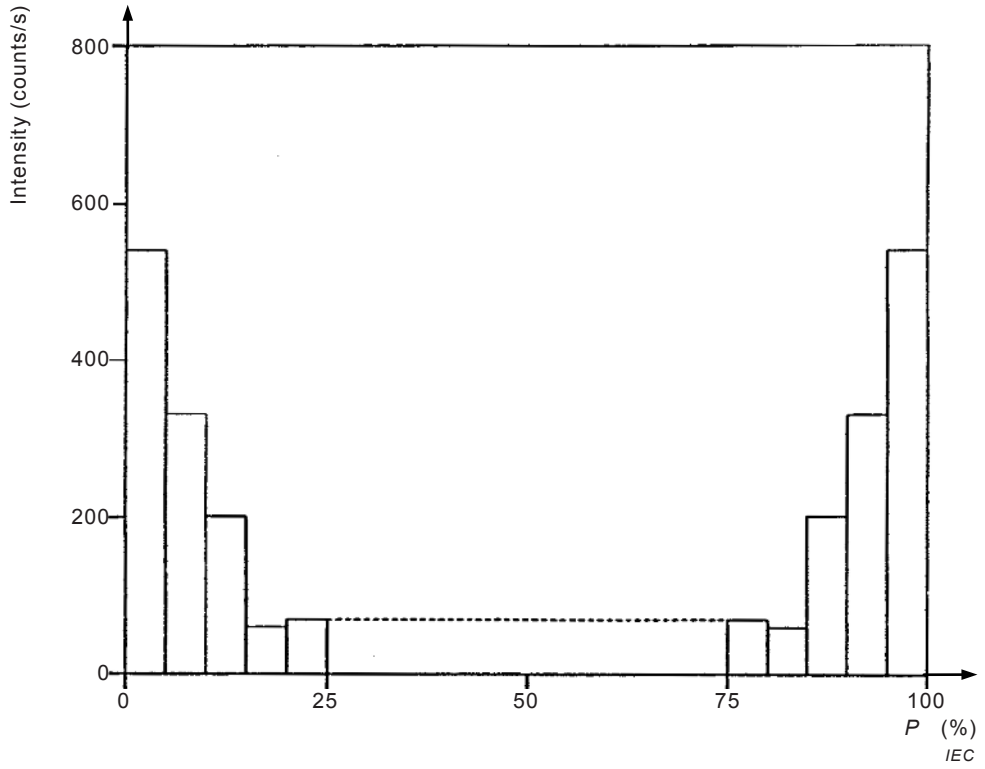

Figure 13 – Chemiluminescence profile for a polypropylene material after gamma irradiation in air to 0,05 MGy at 2 kGy/h (data from [30])

3 Theoretical treatments of diffusion-limited oxidation

Diffusion-limited oxidation can result whenever oxidation reactions in a material use up oxygen faster than it can be replenished by diffusion effects from the air surrounding the material. Thus, theoretical modelling of diffusion-limited oxidation profiles necessitates combining diffusion equations with expressions for the rate of oxygen consumption, the latter derived from the kinetics appropriate to the oxidation of the material. A particularly useful theoretical treatment of diffusion-limited oxidation for slabs of material of thickness, L, was originally formulated by Cunliffe and Davis [5] using oxidation kinetics which are terminated by bimolecular reactions. More recently, Gillen and Clough [6, 7, 22, 23] showed that very similar theoretical results occur for oxidation kinetics which are terminated by unimolecular reactions. Details of the derivations are given in Annex A.

The profiles derived from these theoretical approaches depend upon two parameters, α and β, given by:

$$\alpha = \frac{\left(C_1 L^2\right)}{D} \tag{1}$$

$$\beta = C_2 S p = C_2 [O_2]_e \tag{2}$$

where

L is the slab thickness;

C_1 and C_2 are constants involving the kinetic rate constants underlying the chemical degradation;

D and S are the diffusion and solubility parameters for oxygen in the material;

p is the oxygen partial pressure of the surrounding atmosphere; and

$[O_2]_e$ denotes the oxygen concentration at the edge of the sample.

Representative theoretical profiles for the normalized oxidation of sheet material exposed on both sides to oxygen are shown in Figures 14, 15 and 16 [5, 6, 7, 23]. P gives the percentage of the distance from one oxygen-exposed surface of the sheet to the opposite oxygen-exposed surface. For small values of β, we find "U-shaped" oxidation profiles; when β is large, the profiles are "step-shaped" with abrupt transitions between oxidized and unoxidized regions of the samples. For intermediate values of β, profile shapes of intermediate character result. Comparison of the theoretical shapes with the experimentally derived profiles shown earlier indicates that, in general, the theories have the flexibility to represent the various shapes of profiles observed.

If experimental data can be used to generate values of the two model parameters α and β, the following theoretical relationship [5], derived in Annex A, can be tested:

$$\frac{\left(R_o L^2\right)}{p P_{ox}} = \frac{\alpha}{\beta + 1} \tag{3}$$

where

R_o represents the equilibrium oxygen consumption rate, and

P_{ox} is the oxygen permeation rate (equal to D times S) through the material.

We can also use this equation to calculate the critical thickness L_c, below which the integrated oxidation across the sample will be greater than 90 % of a homogeneously oxidized case. We accomplish this by determining the required value of α_c (the α value corresponding to 90 % integrated oxidation) versus β:

$$\frac{(R_o L^2)}{pP_{ox}} = \frac{\alpha_c}{\beta + 1} \tag{4}$$

Values of $\alpha_c/(\beta + 1)$ are plotted versus β in Figure 17; they vary from ~1,3 at low values of β to ~10 at high values. If we define $C_c = \alpha_c/(\beta + 1)$, Equation (4) can be rewritten as:

$$L_c = \left[\frac{C_c\ pP_{ox}}{R_o}\right]^{0,5} \tag{5}$$

If an appropriate value of C_c can be selected, Equation (5) allows us to use estimates and/or measurements of R_o and P_{ox} (see Clauses 4 and 5 below) to calculate the approximate upper limit on sample thickness if significant diffusion effects are to be avoided. It is clear from the results of Figure 17, that even for the currently discussed theory, no single value of C_c can be specified in Equation (5). Many researchers [5, 16] have set C_c equal to 8 in order to estimate L_c, a reasonable choice for large values of β ("step-shaped" profiles); others [31] have set it equal to 1, a value clearly appropriate for very small values of β ("U-shaped" profiles). By settling on a single value of this quantity in the absence of profile shape information, this provides a simple equation allowing for the estimation of the importance of diffusion effects. An intermediate value of 4 gives:

$$L_c = 2\left[\frac{pP_{ox}}{R_o}\right]^{0,5} \tag{6}$$

an equation which will be utilized and tested in Clause 6. Although selecting $C_c = 4$ might seem like an arbitrary choice, it turns out to give reasonable guarantees that samples are homogeneously oxidized, regardless of the profile shape. In the worst case situation of very low values of β, the integrated oxidation across the sample will be greater than 75 % of that appropriate to a homogeneously oxidized sample. Equation (6), therefore, should offer a reasonably general expression for estimating L_c, regardless of the precise details of the underlying oxidation kinetics.

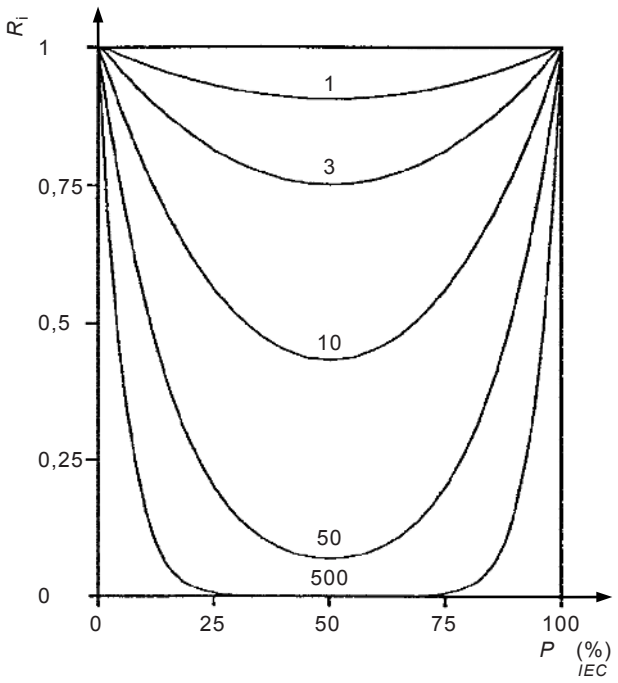

NOTE *P* represents the percentage of the distance from one oxygen-exposed surface of the slab of material to the opposite oxygen-exposed surface (from [7, 23]).

Figure 14 – Theoretical oxidation profiles for various values of α (indicated in the figure) with β = 0,1

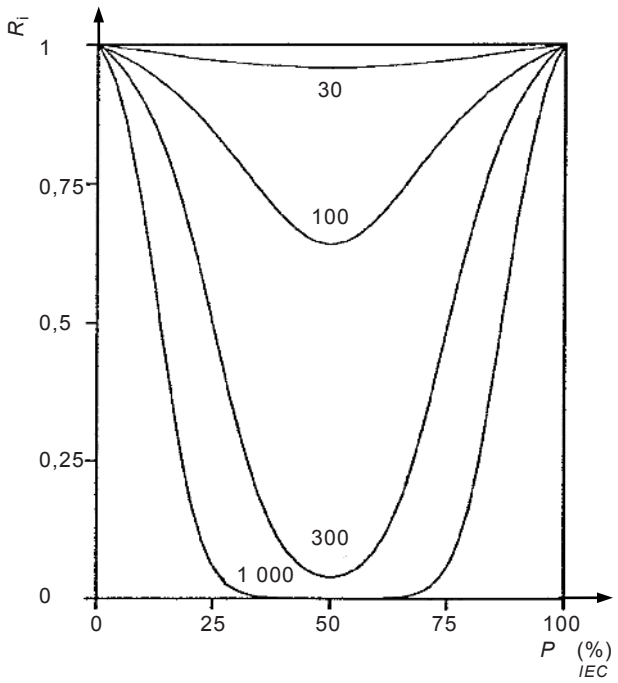

Figure 15 – Identical to Figure 14, except that β = 10

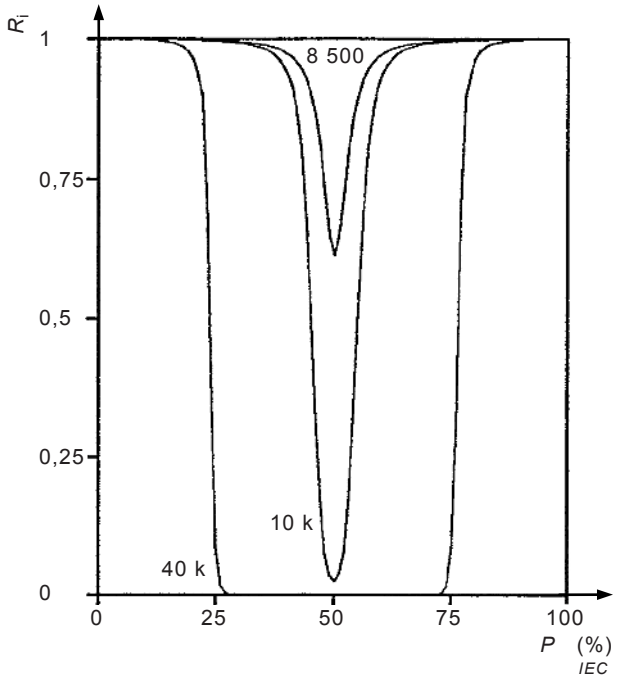

Figure 16 – Identical to Figure 14, except that β = 1 000

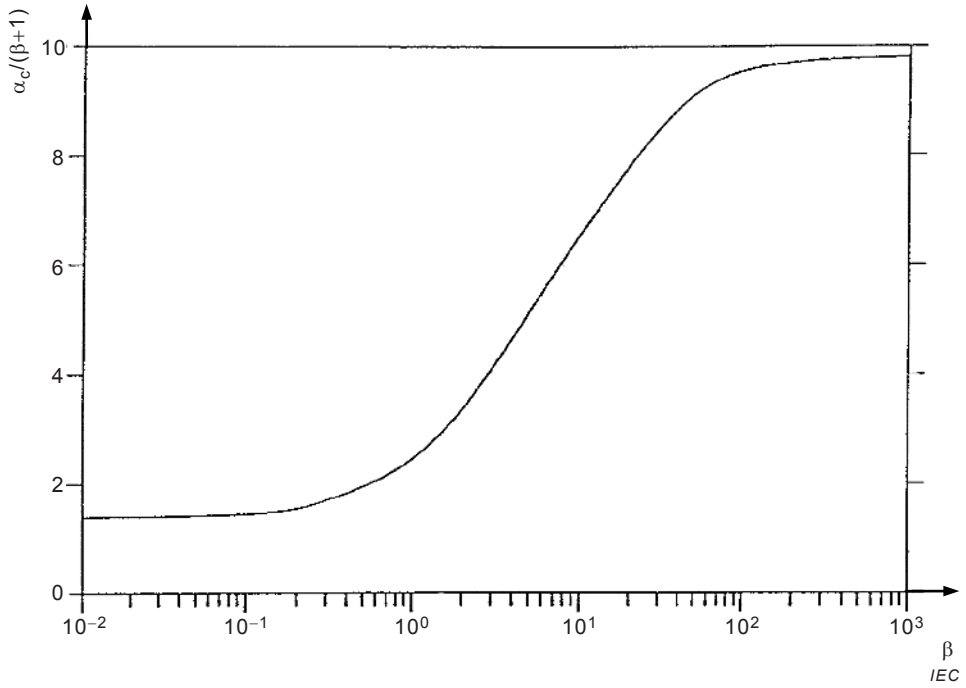

Figure 17 – Plot of $\alpha_c/(\beta + 1)$ versus β, where α_c denotes the value of integrated oxidation corresponding to 90 % (from [7, 23])

4 Permeation measurements

In order to use Equation (6) to estimate the importance of diffusion effects, one needs an estimate of P_{ox}, the oxygen permeability coefficient for the material. Since P_{ox} equals the product of D and S, knowledge of these quantities (the oxygen diffusion and solubility coefficients, respectively) would be equivalent. Fortunately, measurements of these three parameters for oxygen in polymers has been going on for many years, so there is a very large literature describing experimental techniques and data for numerous polymeric materials. There are numerous good reviews and papers, of which a few will be noted [1, 9, 32 to 37]. It is usually possible to obtain an estimate of the oxygen permeability coefficient through the use of a literature search; if literature values are not available, commercially available instruments or analytical service companies can be used to obtain experimental results for a material of interest.

5 Oxygen consumption measurements

Many earlier measurements of the oxygen consumption rate, R_o, for materials were made by monitoring the pressure drop of an oxygen atmosphere surrounding the material during ageing (so-called "oxygen uptake measurements"). This approach is much more difficult to apply in high energy radiation ageing environments. More important, this technique can easily underestimate the true oxygen uptake, since reaction of the material with oxygen usually leads to the generation of gaseous products, thereby reducing the pressure drop.

More modern approaches use analytical techniques which quantify the amount of oxygen before and after ageing. For instance, a typical approach [38 to 40] involves placing a measured amount of a powdered or thin film polymer in a glass ampoule (known volume) with a break-off seal. The ampoule is filled with a measured amount of oxygen, sealed and then aged in the environment of interest. After ageing, the gases remaining in the ampoule are analysed by gas chromatography. This allows estimates to be made of both the oxygen consumed and of the gases produced from the degradation of the polymer. In carrying out the experiments, it is important to have small enough sample dimensions so that the consumption measurements are being made in the absence of diffusion-limited oxidation. After an

experiment is completed, Equation (6) can be used, together with an estimate or measurement of the permeability coefficient, Pox, to verify that diffusion effects were absent.

As shown in Annex A, even in the absence of diffusion effects, the oxygen consumption rate can depend on the oxygen partial pressure surrounding the sample. This implies that either the average of the initial and final partial pressures in the ampoule should approximate the partial pressure of interest (usually that of air), or that a lack of dependence on partial pressure is verified. For radiation environments, again in the absence of diffusion effects, it should be cautioned that the oxygen consumption rate per Gy of absorbed dose may depend on dose rate [38, 40]. This means that either the lack of dose-rate effects has to be verified, or measurements made at the dose rate of interest to the ageing or modelling.

6 Comparison of theory with experimental results

The oxidation profile theories summarized earlier in Clause 3 are now quantitatively tested [22, 23] (see Annex A for more detailed discussion of the theories). Since the theories assume steady-state conditions, systems in which R_o and P_{ox} (the oxygen consumption and permeation rates, respectively) are relatively constant with ageing time shall be chosen.

This situation often occurs in high energy radiation environments. For example, in gamma-initiated oxidations of commercial elastomers, R_o is often relatively constant up to moderate total radiation doses (0,5 MGy to 1 MGy) [7, 15]. In addition, P_{ox} seldom changes by more than 10 % to 20 % for doses of 0,5 MGy [9]. The EPDM material of Figure 9, which was aged to 0,32 MGy at 6,65 kGy/h and 70 °C, met these criteria [22, 23]. Since the density changes plotted in Figure 9 are predominantly caused by oxidation, the profile results for the two thicknesses (0,302 cm on the left, 0,18 cm on the right) were fitted with the theory described in Clause 3. The best theoretical fits to the experimental data occur for $\beta = 6$, together with $\alpha = 154,5$ (0,302 cm thick sample) and $\alpha = 55$ (0,18 cm thick sample). These calculated profiles are shown as the solid curves in Figure 9. Note that this is a two-parameter fit, since the two values of α shall be related by the ratio of the squares of the sample thicknesses, as seen from Equation (1). It is clear from the results that the theory does an excellent job of characterizing the profile shapes and their dependence on L. The resulting values of α and β from the fitting procedure yield for the thick sample:

$$\frac{\alpha}{\beta+1} = 22,1 \pm 3 \tag{7}$$

Separate experiments on the same EPDM material measured the oxygen consumption rate (R_o) as $(5,6 \pm 0,2) \times 10^{-10}$ moles O_2/Gy/cm^3 and found that oxygen permeation rate (P_{ox}) at 70 °C was $(2,4 \pm 0,2) \times 10^{-14}$ mol/(mPas). These results, coupled with an oxygen partial pressure of 17,6 kPa, give the following for the 0,302 cm thick sample on the left-hand side of Equation (3):

$$\frac{R_o L^2}{pP_{ox}} = 22,2 \pm 3 \tag{8}$$

Since this independently calculated result is equal to the result found above in Equation (7), the fit is quantitatively consistent with the theoretical relationship given by Equation (3).

Now that some confidence in the theoretical modelling has been developed, it is interesting to test Equation (6), the theoretical expression for estimating the approximate oxidative penetration distance. For the radiation-aged EPDM sample, Equation (6) gives an L_c of 1,27 mm. For the 3,02 mm thick sample (left side of Figure 9), this implies an "oxidative penetration depth" reaching ~21 % of the way in from each air-exposed surface; for the 1,8 mm sample (right plot), a depth of ~35 % from each side is predicted. If a sample of thickness equal to ~L_c (1,27 mm) were aged, the full theory ($\beta = 6$, $\alpha = 27$) would predict that the integrated oxidation would be ~90 % of a homogeneously oxidized case. For the commercial

fluoro elastomer material of Figures 5 to 7, R_O is approximately constant and equal to $7,5 \times 10^{-10}$ mole O_2/Gy/cm^3 over the entire dose range of 0 MGy to 1,05 MGy and $P_{ox} \cong 5,0 \times 10^{-15}$ mol/(mPas) [15]. This leads to an L_c of 0,55 mm at 5,49 kGy/h, which corresponds to a predicted ~17 % penetration of the oxidation in Figure 5. At 0,9 kGy/h, L_c increases to 1,36 mm or a predicted 40 % penetration for the data of Figure 6. Comparing the results from Equation (6) with the experimental profiles, it is clear that approximate relationships such as Equation (6) can be very useful for estimating the thickness of sample necessary for eliminating diffusion-limited oxidation effects if estimates or measurements of oxygen permeation and consumption rates are available.

It is also interesting to note that the experimental profiling results for the commercial fuoro elastomer material imply that the "oxidative penetration distance" is approximately independent of dose. Since R_O is also found to be independent of dose [15], this implies that P_{ox} does not change dramatically with dose, a result consistent with many other elastomers aged in radiation environments [9].

Finally, it is instructive to apply Equation (6) to the early stages of the thermal ageing results for the chloroprene rubber material described in Figure 8. At 150 °C, the measured value of R_O for the first day of ageing is $6,7 \times 10^{-3}$ mol/(m^{3}s) [10]. Although P_{ox} drops dramatically with ageing time, the drop is minor in the first day, so we can estimate that at 150 °C, P_{ox} equals approximately $7,7 \times 10^{-14}$ mol/(mPas) [10]. This leads to an L_c estimate of 0,89 mm, which corresponds to ~22 % oxidative penetration from each side of the sample, in reasonable agreement with the experimental result after 1 day of ageing. Assuming typical activation energies of 84 kJ/mol and 42 kJ/mol, respectively for R_O and P_{ox}, we estimate that L_c equals ~2 mm for the early stages of thermal ageing at 100 °C. This implies initially homogeneous oxidation, in agreement with the experimental results given in Figure 8. Later on, at both temperatures, diffusion-limited oxidation becomes more important, primarily due to a significant decrease in P_{ox} caused by the hardening of the material [10].

7 Oxygen overpressure technique

Another interesting approach that can be used to eliminate diffusion-limited oxidation effects is the so-called oxygen overpressure technique, which was pioneered for radiation environments by Seguchi and co-workers [41, 42, 43]. Their apparatus for carrying out such experiments is shown in Figure 18 [43]. It consists of a pressure vessel connected to an oxygen source with a pressure regulator and protected with safety equipment, such as safety valves or rupture discs. In radiation environments, the gases evolved from reacting samples has to be removed from the vessel for total doses above approximately 0,1 MGy; one method of accomplishing this is to have a continuous leak of the gases (oxygen and product) during irradiation. Because of safety considerations, it is recommended that the oxygen pressure be kept below 1 MPa. The pressure vessel is also temperature controlled. Again, because of safety considerations, they recommend that the temperature of the samples during irradiation be kept below 50 °C for pure polymers and 70 °C for formulated polymers (thermal oxidation in pressurized oxygen occurs at lower temperatures than it does in air).

From Equation (5), it is clear that increasing the oxygen pressure p, surrounding the sample will result in larger values of L_c, and therefore reductions in diffusion-limited oxidation effects. Since p ~0,02 MPa for air environments, an oxygen overpressure experiment at ~1 MPa will increase L_c by a factor of ~7 times. As discussed above, the value of C_c in Equation (5) will depend on the value of β appropriate to the experiment (see Figure 17). For radiation ageing under air environments, most evidence (see for example Figures 2, 5, 6, 9, 10, 12 and 13) indicates intermediate values of β (e.g. from 3 to 100). Since β is proportional to p (see Equation (2)), typical high-pressure oxygen experiments (0,2 MPa to 1 MPa) will increase β by factors of 10 to 50. Thus the β values appropriate at high oxygen pressures should be in the range of 30 to 5 000, implying that C_c in Equation (5) would be equal to 9 ± 1, consistent with the value of 8 used by Seguchi and co-workers in their analyses [8, 42]. It should be noted that when β is small to intermediate under air-ageing conditions, raising the oxygen pressure can lead to increases in oxidation at the sample edges, in addition to increasing the oxidative penetration distance into the sample (see Annex A). In such instances, increasing the oxygen

pressure to eliminate diffusion-limited oxidation effects will eventually result in uniform oxidation throughout the sample, but at a level higher than would occur under air-ageing conditions. Only when evidence exists that the edge oxidation or equivalently the G-values for oxygen consumption (in radiation environments) is insensitive to oxygen pressure (e.g. for 0,02 MPa and higher) can the overpressure technique be rigorously used to eliminate diffusion effects. Seguchi and co-workers [38] addressed this issue and confirmed that G-values for oxygen consumption are constant for a number of unstabilised materials over a wide range of oxygen pressures. This implies that the β values for these materials in air are relatively large (e.g. greater than 10).

For radiation-aged materials where chemical dose-rate effects are unimportant (e.g. in the absence of diffusion effects, degradation depends only on the dose, not the dose rate), the oxygen overpressure technique can be used to eliminate diffusion effects at high dose rates and therefore allow lower dose-rate predictions to be made. Figure 19 shows, for example, elongation and tensile strength data for an EPR cable insulation material which was aged at high and low dose rates in air and at a high dose rate in pressurized oxygen. The dose-rate effect observed under the air ageing conditions, caused by the presence of diffusion-limited oxidation at the high dose rate, is eliminated by conducting a high dose-rate experiment in pressurized oxygen.

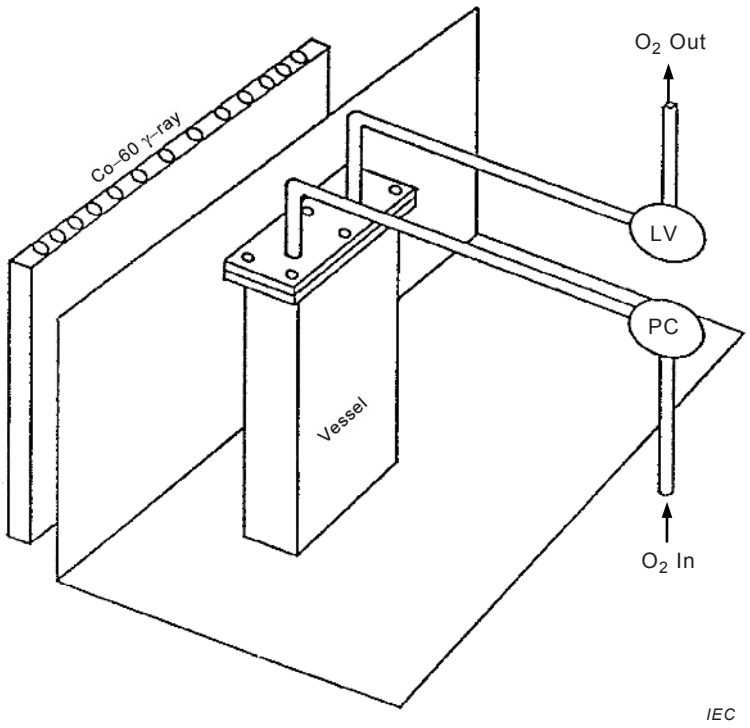

NOTE PC is a pressure regulator, LV is a leak valve (from [43]).

Figure 18 – Apparatus used for irradiation under pressurized oxygen conditions

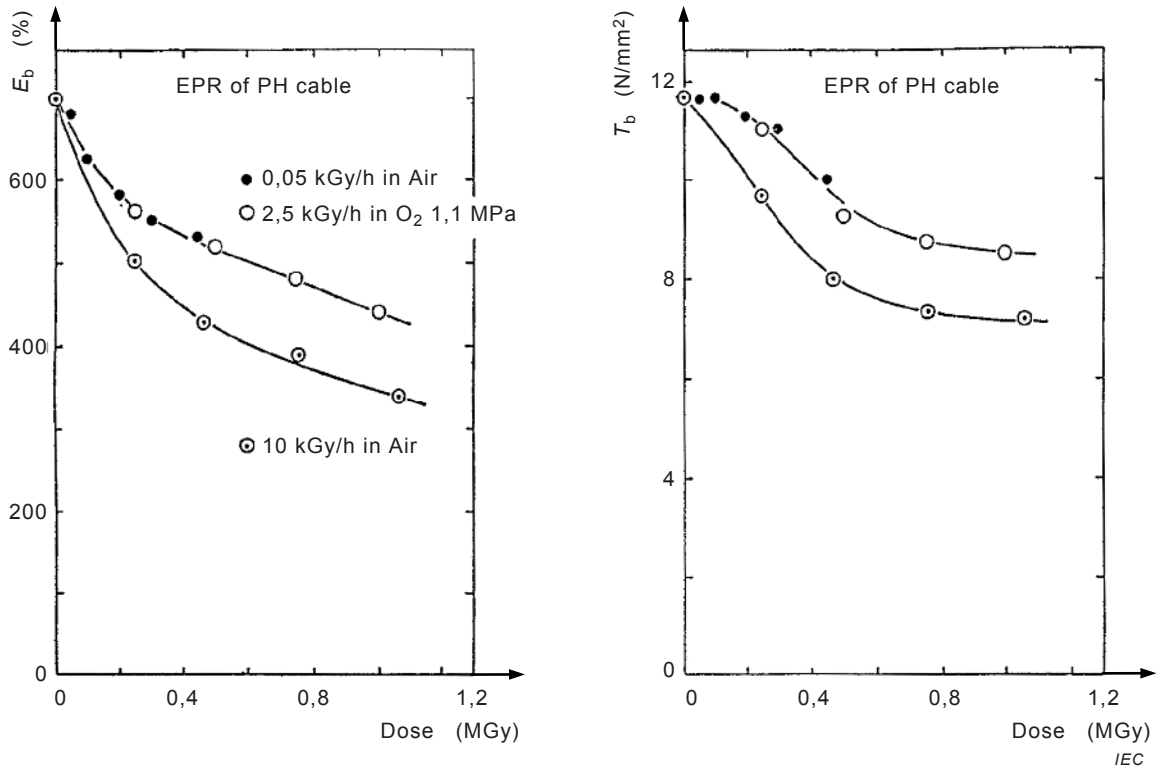

Figure 19 – Tensile elongation (left) and tensile strength (right) data for an EPR material aged at the indicated high and low dose-rates in air and at high dose rate in the pressurized oxygen apparatus of Figure 18

8 Summary

It should be clear, given the examples shown in this technical specification, that diffusion-limited oxidation effects are commonly observed for polymers aged in air in various environments including thermal, high-energy radiation and ultraviolet. Since these effects can complicate both attempts to understand the oxidative degradation mechanisms and attempts at extrapolating short-term accelerated ageing exposures to long-term ageing conditions, they must be monitored and understood or eliminated/minimized. Advances in the development of experimental profiling techniques and in theoretical modelling of the profile shapes now make these goals attainable. A number of the most useful experimental profiling techniques are briefly described in this technical specification. These can be very useful for determining the importance of diffusion effects and monitoring their dependence on experimental ageing conditions. Simplified theoretical models are outlined and the predictions from the models are compared to experiment data. The results of such comparisons lend confidence in the theoretical simulations. Such confidence implies that simple expressions such as Equation (6) can be used to estimate, before ageing experiments are begun, the critical combination of sample thickness and accelerating stress level necessary for eliminating diffusion effects. This will help eliminate extraneous and difficult to interpret experimental exposures. Confirmation that diffusion effects are unimportant can then be accomplished using various experimental profiling techniques.

Annex A
(informative)

Derivation of theoretical treatment of diffusion-limited oxidation

A.1 General

The development of theoretical models requires one to combine diffusion relationships with expressions for the oxygen consumption rate in the polymer during ageing. Rigorous derivations of oxygen consumption rates would necessitate detailed knowledge of the complex kinetics underlying the oxidation processes in polymers, an unrealistic goal. In the interest of deriving tractable kinetic expressions, most attempts at modelling oxidation assume that the generic oxidation scheme [44, 45] shown in Figure A.1 represents a first-order approximation for the oxidation of organic materials, induced by a variety of different stresses (thermal, mechanical, UV light, ionizing radiation, etc.). The main differences occur in the details of the initiation step which first produces the free radical species. It is usually easiest to control the initiation rate in the gamma-initiated case, since R_i is typically independent of ageing time, and linear with the radiation dose rate. In addition, branching reactions, which often enter and complicate the oxidation processes occurring at the high temperatures used for thermal oxidation studies, are often unimportant for lower-temperature, gamma-initiated oxidation. Any growth in importance of branching reactions with ageing time will cause the oxidation rate to increase with time during thermal ageing studies, further complicating attempts to quantitatively model diffusion-limited oxidation. For these reasons, gamma-initiated oxidation appears to represent the simplest possible experimental situation for initial attempts at quantitatively testing diffusion-limited oxidation models. Complications, such as those caused by branching reactions and time-dependent oxidation rates, would then have to be dealt with once confidence existed in the models derived for the simpler experimental situations.

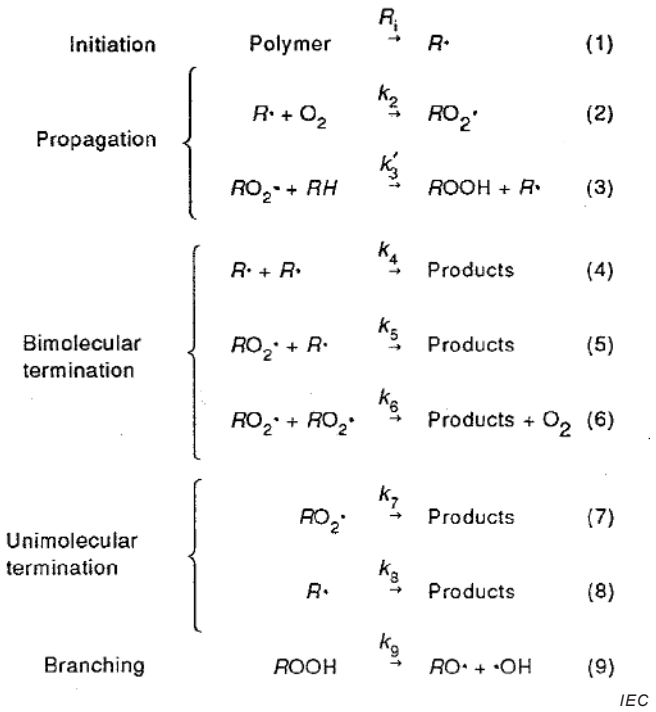

Figure A.1 – Simplified kinetic scheme used to represent the oxidation of polymers (from [44, 45])

For gamma-initiated oxidations involving moderate temperatures and time periods, it will be assumed therefore that the chemistry is adequately represented by reactions (1) to (8) in

Figure A.1. The scheme involving the bimolecular termination steps (reactions (1) to (6)), originally derived for the oxidation of organic liquids, has been invoked for many years for explaining the oxidation of polymers. Using a steady-state analysis, and assuming long kinetic chain lengths (many propagation cycles compared to termination reactions), and $k_5^2 = 4\ k_4\ k_6$, the oxygen consumption rate is given by [44]:

$$\frac{\mathrm{d}O_2}{\mathrm{d}t} = \frac{C_{1b}[O_2]}{1 + C_{2b}[O_2]} \tag{A.1}$$

where

$$C_{1b} = \frac{k_2\, R_i^{0,5}}{(2\ k_4)^{0,5}} \quad \text{and} \quad C_{2b} = \frac{k_6^{0,5}\, k_2}{k_4^{0,5} k_3} \tag{A.2}$$

and $k_3 = k'_3\ [R\mathrm{H}]$.

For many polymeric materials, unimolecular termination reactions are often found to be dominant. For instance, in the presence of sufficient antioxidant, the radical species ($RO_2\cdot$ and $R\cdot$) can terminate in pseudo first-order reactions, yielding an oxidation scheme consisting of reactions (1) to (3) plus (7) and (8). The rate of oxidation is then given by [6, 7, 15]:

$$\frac{\mathrm{d}O_2}{\mathrm{d}t} = \frac{C_{1u}[O_2]}{1 + C_{2u}[O_2]} \tag{A.3}$$

where

$$C_{1u} = \frac{k_2 R_i}{k_8} \quad \text{and} \quad C_{2u} = \frac{k_2\ k_7}{k_8(k_3 + k_7)} \tag{A.4}$$

It is clear from Equations (A.1) and (A.3) that the oxygen consumption rates for the unimolecular and bimolecular schemes have identical functional dependencies on the oxygen concentration. However, the constants in the expressions differ, especially in their dependence on the initiation rate, R_i. For the unimolecular case, the oxygen consumption rate depends upon the first power of R_i, whereas it depends on R_i to the one-half power for the bimolecular case. Thus, if reliable data at various well-characterized initiation rates were available, one could distinguish between the two schemes.

By assuming that the oxygen consumption rate and the oxygen permeability coefficient are independent of time, Cunliffe and Davis [5] used the bimolecular kinetic expression for oxygen consumption, and showed that it could be combined with diffusion expressions to derive theoretical oxidation profiles for slabs of material of thickness L. Assuming one dimensional diffusion (L much smaller than the other two slab dimensions), Fickian behaviour and steady-state conditions with the x-coordinate aligned along the thickness direction:

$$D\frac{\mathrm{d}^2[O_2(x)]}{\mathrm{d}x^2} = -R[O_2(x)] \tag{A.5}$$

where

$[O_2(x)]$ refers to the concentration of oxygen at the point x;

$R\ [O_2(x)]$ denotes the rate of removal of oxygen by reaction at x; and

D is the diffusion coefficient for oxygen in the material.

Substituting the kinetic modelling results given in either Equation (A.2) or Equation (A.3) for $R\,[O_2(x)]$ yields:

$$D\frac{d^2[O_2(x)]}{dx^2} = \frac{C_1\,[O_2(x)]}{1+C_2\,[O_2(x)]} \tag{A.6}$$

At the surfaces of the sample (x = 0 and L), the oxygen concentration must be given by:

$$[O_2\,(0)] = [O_2\,(L)] = [O_2]_S = Sp \tag{A.7}$$

where the surface (equilibrium) oxygen concentration is assumed to follow Henry's law and will therefore be given by the product of S and p, the solubility of oxygen in the polymer and the oxygen partial pressure surrounding the sample, respectively. Another boundary condition occurring at the centre of the sample is:

$$\frac{d\,[O_2(L/2)]}{dx} = 0 \tag{A.8}$$

Transforming the above with the following reduced variables:

$$X = \frac{x}{L} \quad \text{and} \quad \theta = \frac{[O_2]}{[O_2]_s} \tag{A.9}$$

Cunliffe and Davis [5] showed that Equation (14) could be written as:

$$\frac{d^2\,\theta}{dX^2} = \frac{\alpha\theta}{1+\beta\theta} \tag{A.10}$$

where

$$\alpha = \frac{C_1 L_2}{D} \quad \text{and} \quad \beta = C_2 Sp = C_2\,[O_2]_s \tag{A.11}$$

Although they applied this result to the bimolecular kinetic result (C_1 and C_2 are equal to C_{1b} and C_{2b}, respectively), it is clear that identical results hold for unimolecular kinetics if C_{1u} and C_{2u} are used. The boundary conditions now become θ = 1 at X = 0 and X = 1, and $d\theta/dX$ = 0 at X = 0,5. Numerical methods lead to a family of solutions for the relative (e.g. normalized to the surface value) oxygen concentration versus spatial position. If θ_i refers to the relative oxygen concentration at point i in the sample, combining either Equation (A.2) or Equation (A.4) with the definitions of α and β leads to the following expression for the oxidation rate at point i:

$$R[\theta_i] = \frac{\alpha D\,\theta_i [O_2]_s}{L^2(1+\beta\theta_i)} \tag{A.12}$$

Similarly, the oxidation rate at the surface (R_s), which is identical to the equilibrium oxygen consumption rate, is given by:

$$R_s = \frac{\alpha D[O_2]_s}{L^2(1+\beta)} \tag{A.13}$$

Thus the relative oxidation at point i is given by:

$$R_i = \frac{R[\theta_i]}{R_s} = \frac{\theta_i(1+\beta)}{1+\beta\theta_i} \tag{A.14}$$

The above analysis can be used to derive theoretical oxidation profiles (plots of R_i versus normalized cross-sectional position) and the corresponding profiles of the relative oxygen concentration (θ_i versus position) [6]. Representative R_i results for three values of β and various values of α are given in Figures 14 to 16. By rearranging Equation (A.13) and noting that:

$$D[O_2]_s = pP_{ox} \tag{A.15}$$

where P_{ox} is the oxygen permeability coefficient through the material, the very useful theoretical relationship given by Equation (3) is obtained.

It is also interesting to use the theory to examine the predicted dependence of the oxidation at the surface of the sample on the oxygen partial pressure surrounding the sample. It can be easily seen from either Equation (A.1) or (A.3), plus Equations (1) and (2), that the equilibrium oxygen consumption rate (R_o) or equivalently the oxidation rate at the edge of the material (R_e), is given by:

$$R_o = R_e = \frac{dO_2}{dt} = \frac{C_1[O_2]_e}{1+C_2[O_2]_e} = \frac{C_1 Sp}{1+\beta} \tag{A.16}$$

Thus, if β_r refers to the value of β at a reference oxygen partial pressure, p_r, the ratio of the edge oxidation rate at an oxygen pressure p, to that under reference conditions, is given by:

$$\frac{R_e(p)}{R_e(p_r)} = \frac{1+\beta_r}{\left(p_r/p\right)+\beta_r} \tag{A.17}$$

This implies, for instance, that if β is equal to 3 under air-ageing (0,02 MPa) conditions for a given material, increasing the oxygen pressure surrounding the sample to 1 MPa (10 atm) would lead to a 33 % increase in the rate of oxidation at the surface of the sample.

A.2 Numerical simulation

The basic differential Equation (A.18) for slab specimen, which is derived in the previous clause, is difficult to solve analytically, so the numerical method is applied.

$$\frac{\partial\theta}{\partial T} = \frac{\partial^2\theta}{\partial X^2} - \frac{\alpha\theta}{1+\beta\theta} \tag{A.18}$$

Here, again

$$T = \frac{Dt}{L^2}, X = \frac{x}{L}, \theta = \frac{[O_2]}{[O_2]_s}, \alpha = \frac{C_1 L^2}{D}, \beta = C_2 Sp = C_2[O_2]_s \tag{A.19}$$

Equation (A.18) is digitized as follows:

The normalized position X is digitized into (N+1) points with an interval of $\triangle X$, and the normalized time T is digitized with an interval of $\triangle T$. The normalized concentration of oxygen at position *i* and time *j* can be expressed as $i \neq 0,N$, where $\theta_{0,j} = \theta_{N,j} = 1$

$$\frac{\theta_{i,j+1} - \theta_{i,j}}{\Delta T} = \frac{\theta_{i-1,j} - 2\theta_{i,j} + \theta_{i+1,j}}{(\Delta X)^2} - \frac{\alpha\theta_{i,j}}{1 + \beta\theta_{i,j}} \tag{A.20}$$

$$\theta_{i,j+1} = \theta_{i,j} + \frac{\Delta T}{(\Delta X)^2}\left(\theta_{i-1,j} - 2\theta_{i,j} + \theta_{i+1,j}\right) - \Delta T \frac{\alpha\theta_{i,j}}{1 + \beta\theta_{i,j}} \tag{A.21}$$

An example of simulation code is given in ref [46]. When the difference in concentrations between positions *j* and *j* + 1 decrease below prescribed level, it was assumed the stable states. By using the simulation code, such figures as Figures 14 to 16, R_i at the relative oxidation at point i, as a function of P, % percentage from one surface to the opposite surface, can be obtained.

A.3 Cylindrical and spherical geometries and simulation

In this clause, the shape of specimen is changed from a slab (as described in previous clauses) to a cylinder. The cylindrical shape would be more practical when cable insulation is considered. Further, it may be a natural extension to consider a spherical shape. The Laplacian changes as follows respectively;

For cylindrical shape,

$$\frac{\partial^2\theta}{\partial X^2} \rightarrow \frac{1}{X}\frac{\partial}{\partial X}\left(\frac{\partial\theta}{\partial X}\right) = \frac{\partial^2\theta}{\partial X^2} + \frac{1}{X}\frac{\partial\theta}{\partial X} \tag{A.22}$$

For spherical shape,

$$\frac{\partial^2\theta}{\partial X^2} \rightarrow \frac{1}{X^2}\frac{\partial}{\partial X}\left(X^2\frac{\partial\theta}{\partial X}\right) = \frac{\partial^2\theta}{\partial X^2} + \frac{2}{X}\frac{\partial\theta}{\partial X} \tag{A.23}$$

As similarly in the case of slab, the differential equations are digitized. Typical solutions at the equilibrium are illustrated in Figures A.2 to A.9 [46] for various combinations of alpha and beta.

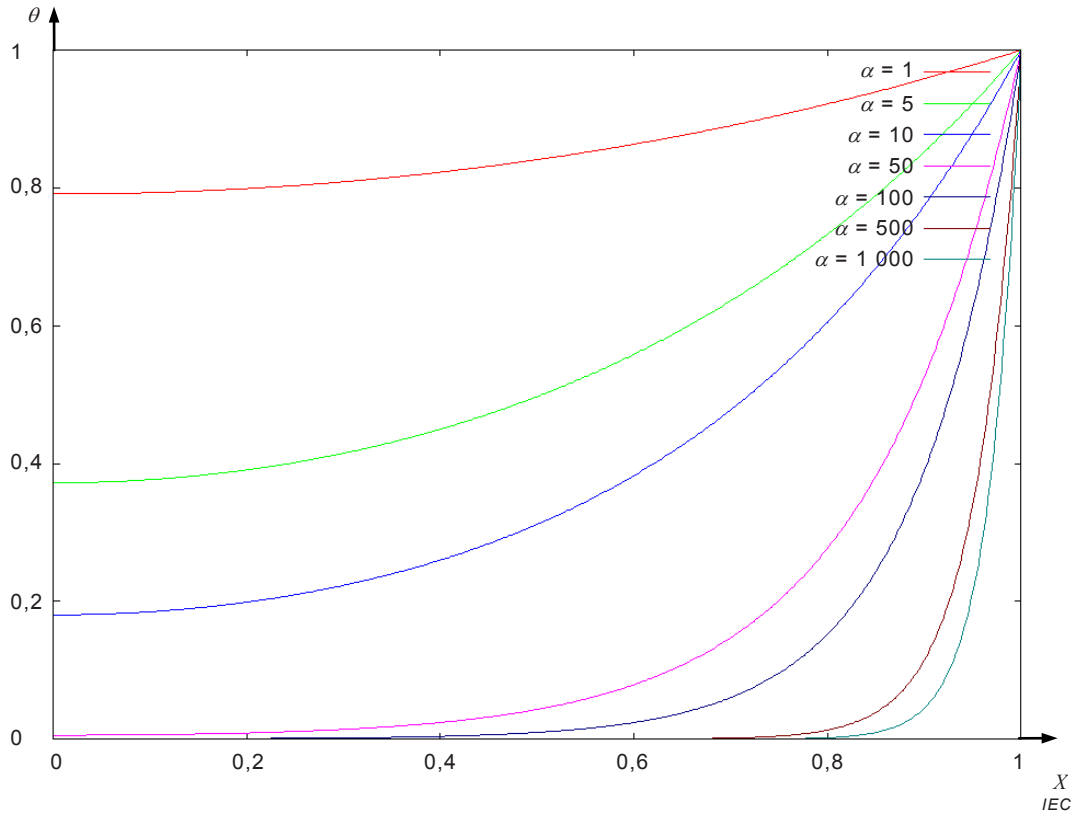

Figure A.2 – Typical example of normalized concentration of oxygen for cylindrical shape for β=0,01 from [46]

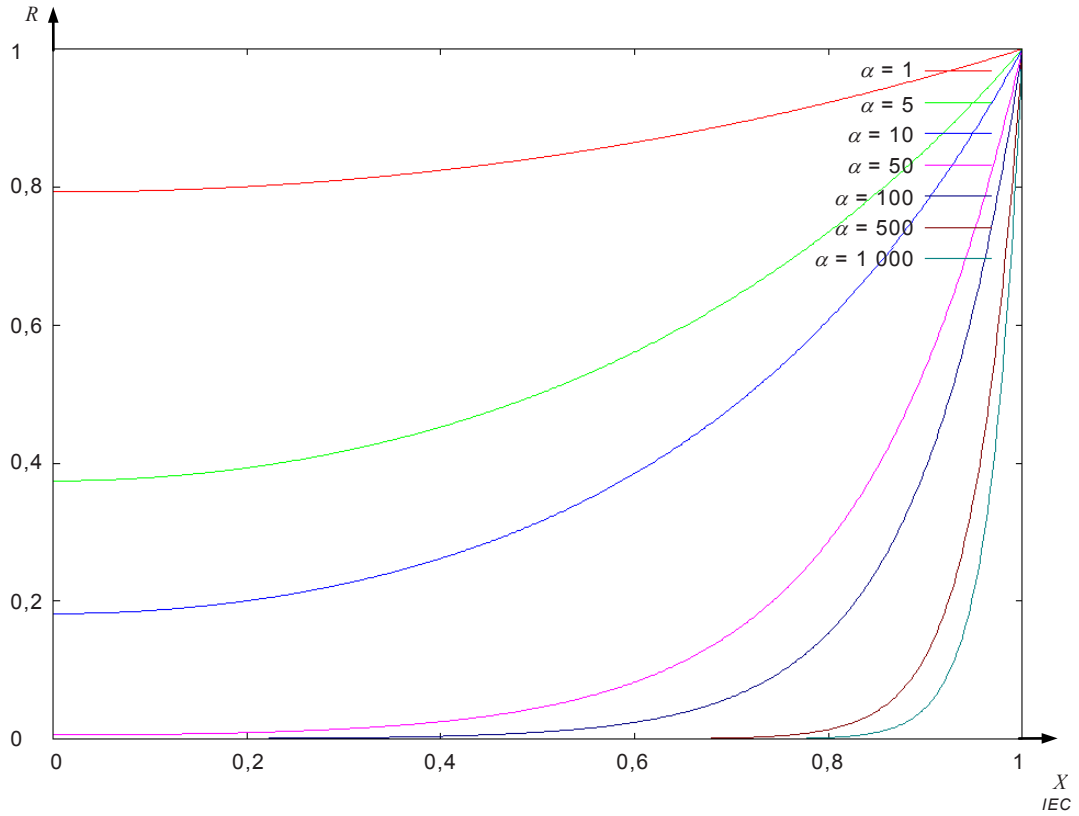

Figure A.3 – Typical example of relative oxygen consumption for cylindrical shape for β=0,01 from [46]

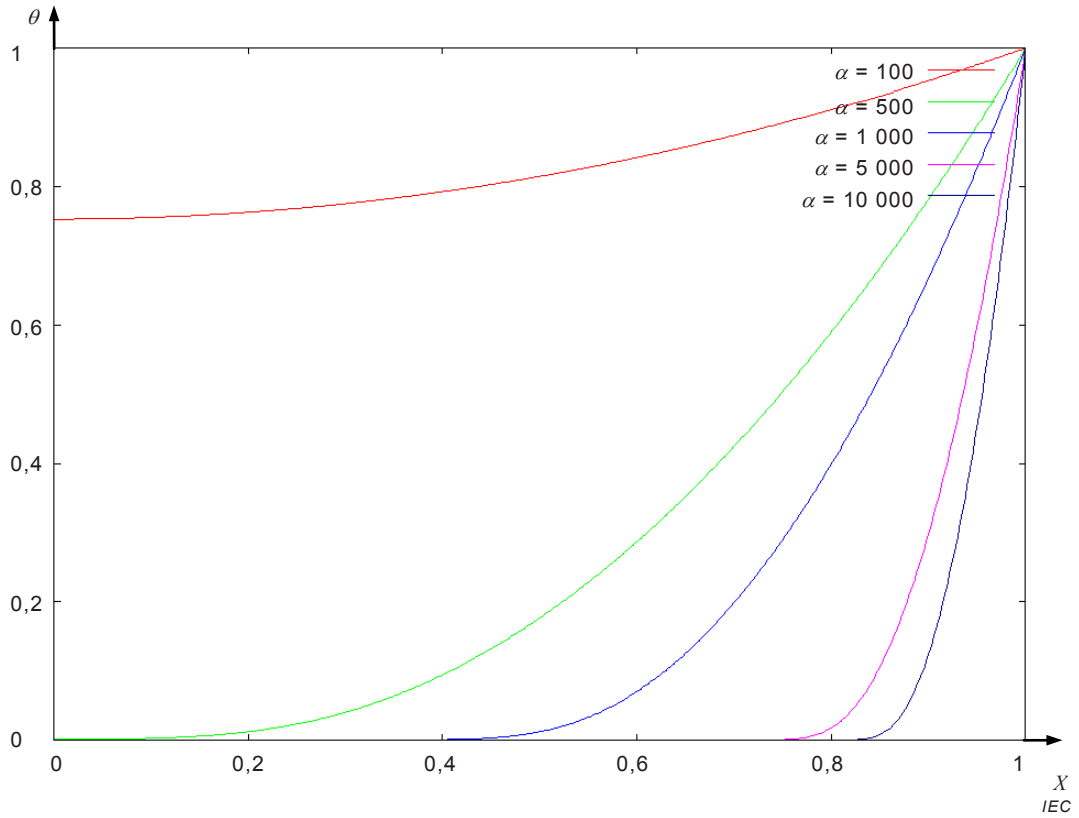

Figure A.4 – Typical example of normalized concentration of oxygen for cylindrical shape for β=100 from [46]

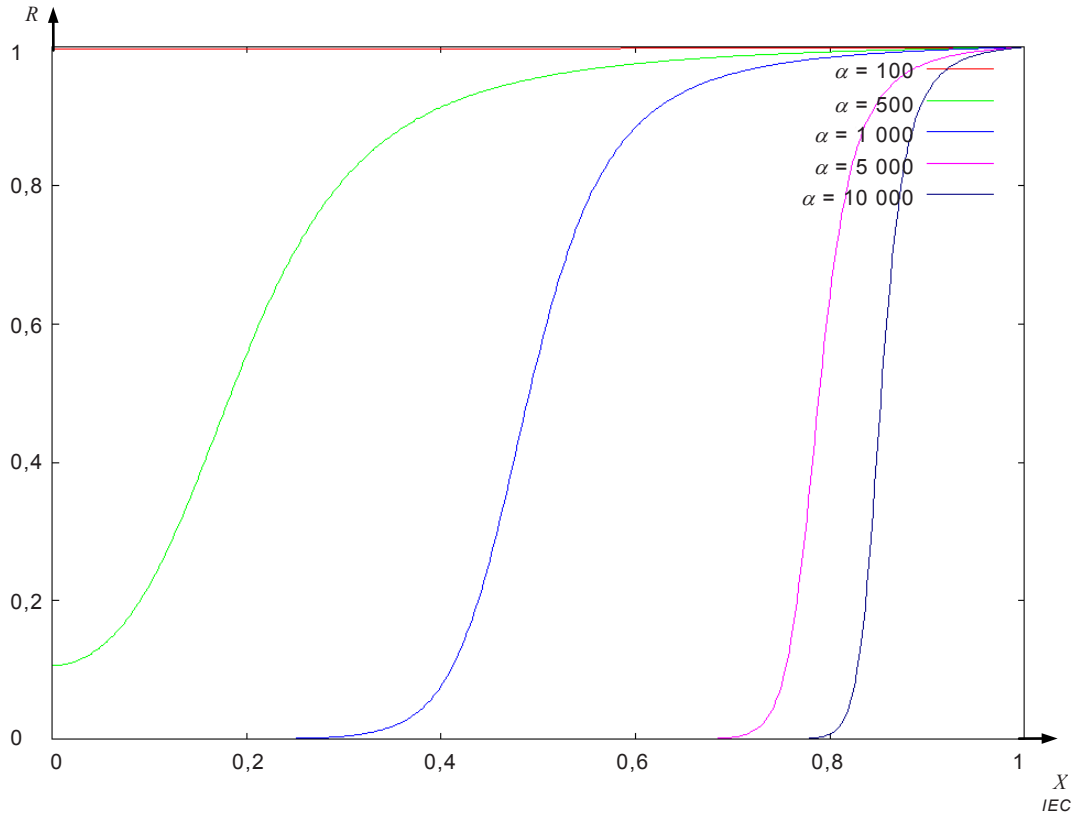

Figure A.5 – Typical example of relative oxygen consumption for cylindrical shape for β=100 [46]

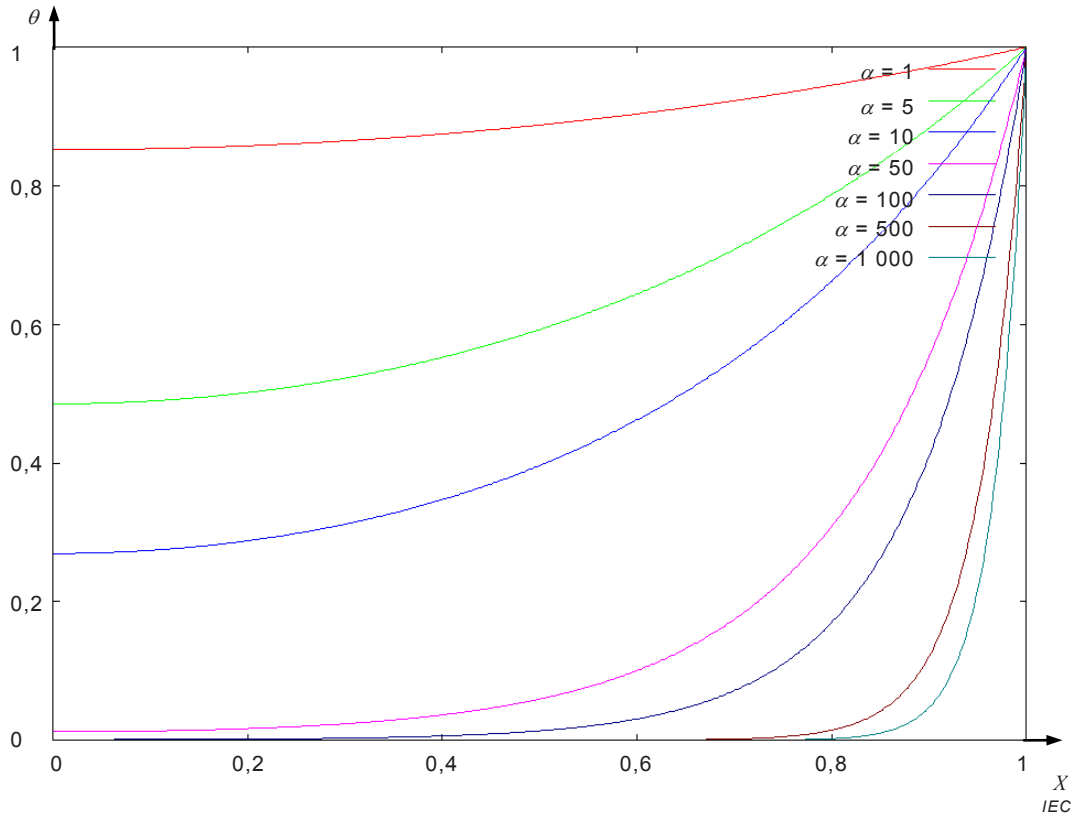

Figure A.6 – Typical example of normalized concentration of oxygen for spherical shape for β=0,01 from [46]

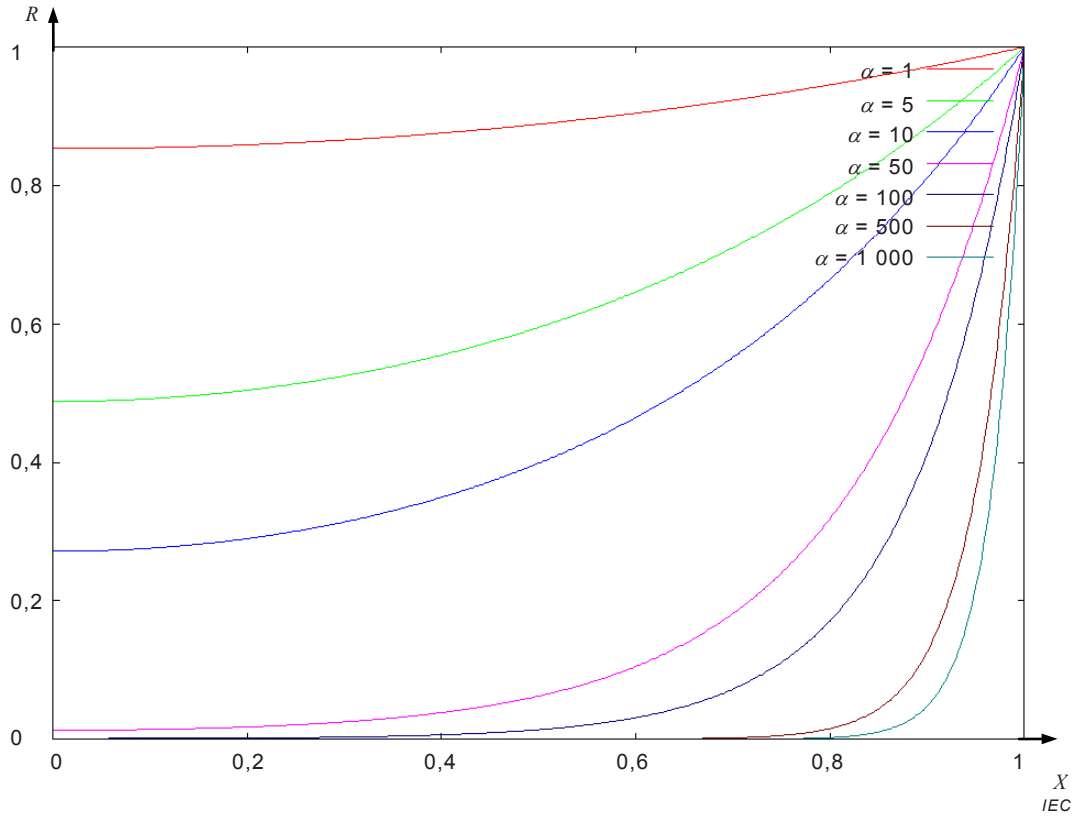

Figure A.7 – Typical example of relative oxygen consumption for spherical shape for β=0,01 from [46]

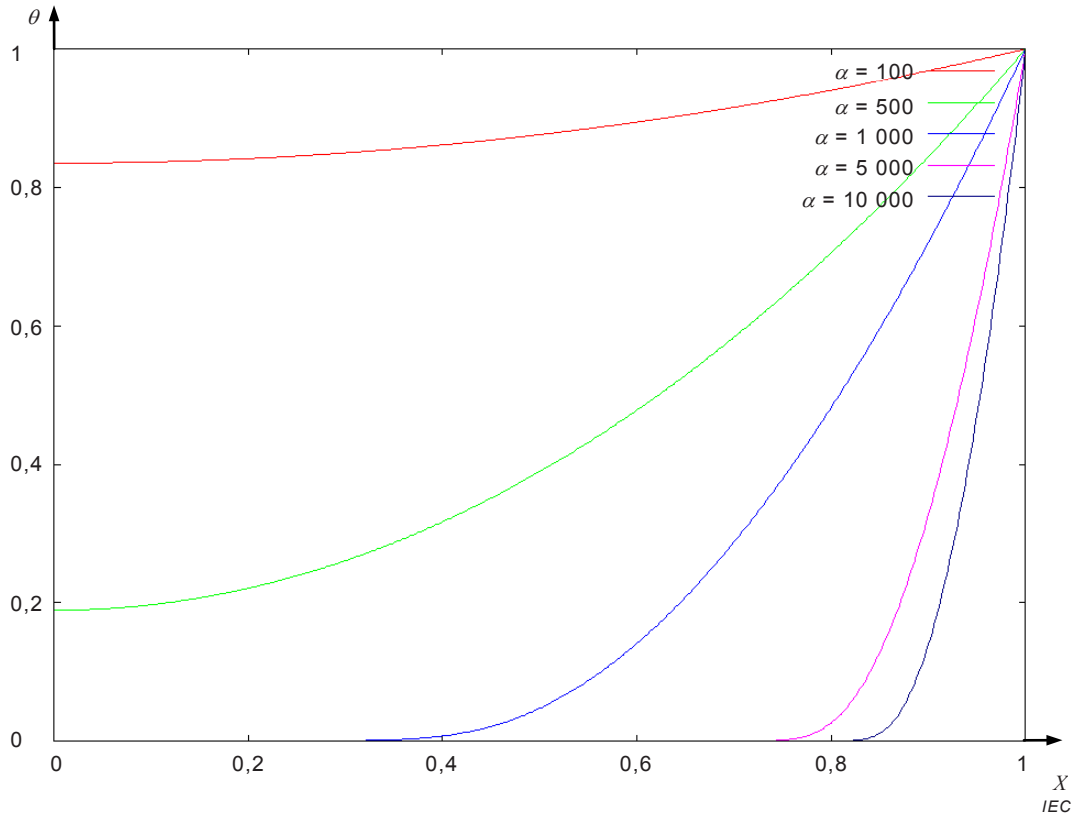

Figure A.8 – Typical example of normalized concentration of oxygen for spherical shape for β=100 from [46]

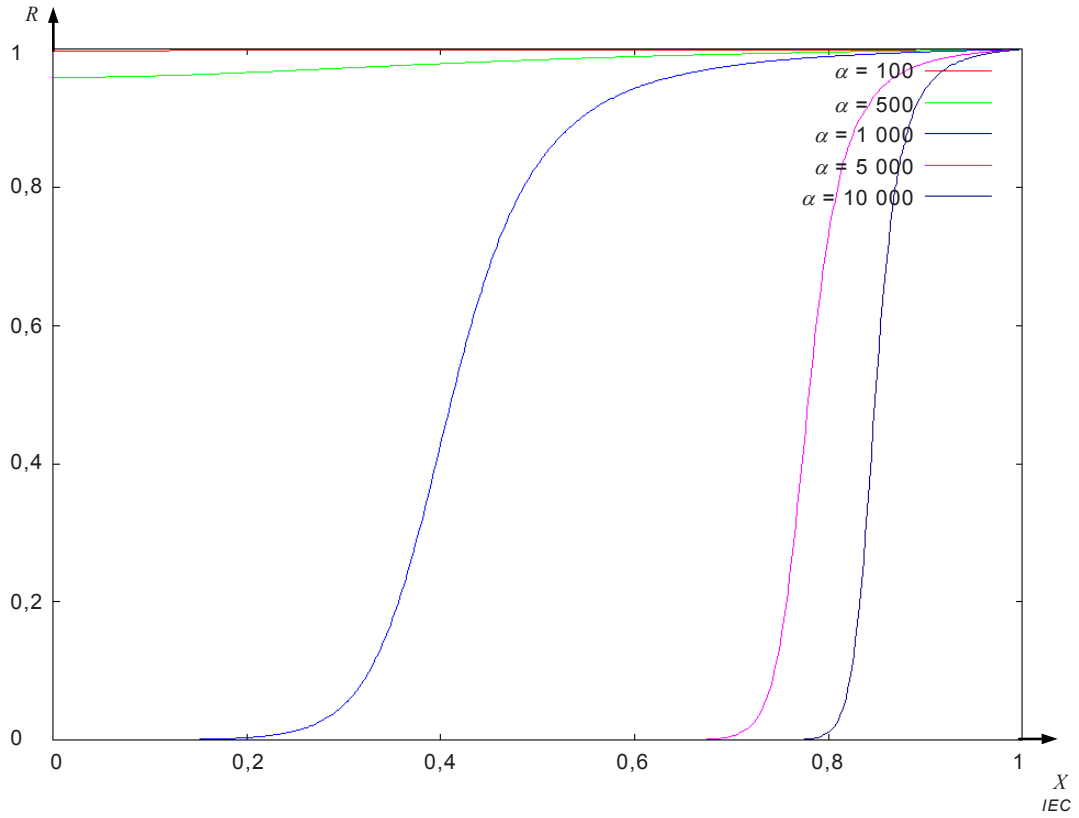

Figure A.9 – Typical example of relative oxygen consumption for spherical shape for β=100 [46]

A.4 Time dependence of the simulation

The general approach has been to handle stable (equilibrium) states. Time-dependent solution is derived as in the simulation code above. The change in normalized concentration of oxygen at the centre is illustrated in Figures A.10 and A.11 [46] for various combinations of alpha and beta.

In order to obtain a rough image on time-scale, an estimation shall be made. In the actual situation, D would range for 10^{-6} – 10^{-7} cm^2/s, and L ranges 1 – several dozens of cm [47], and by considering that $\triangle t=L^2 \triangle T/D$, the time interval $\triangle t$ would become 10^2 –10^5 s.

According to the simulation results, it would take several hundred thousand steps to converge for heterogeneous oxidation, which indicates that it would take around 10^8 s (several years).

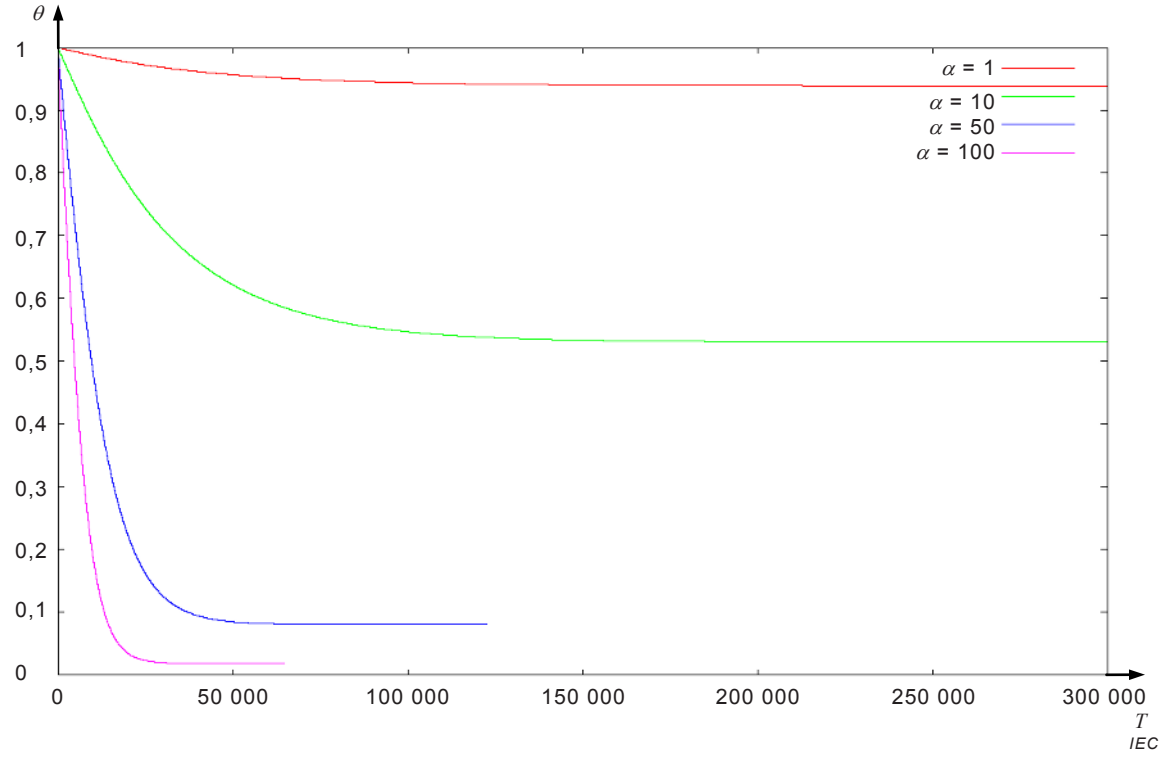

Figure A.10 – Typical example of time-dependent normalized concentration of oxygen at the centre from for the case of β=1 [46]

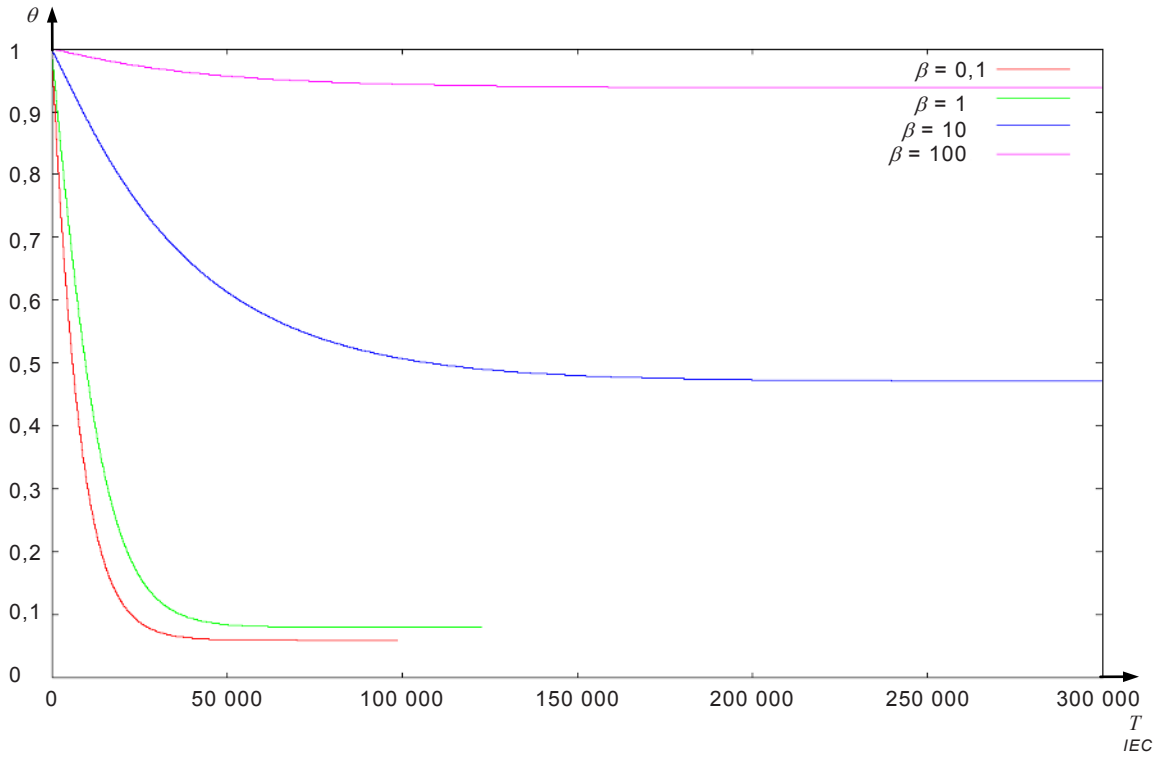

Figure A.11 – Typical example of time-dependent normalized concentration of oxygen at the centre from for the case of α=50 [46]

Bibliography

[1] AMERONGEN, G.J., *Rubber Chem. Tech*., 37, 1065 (1964).

[2] MATSUO, H. and DOLE, M., J. Phys. Chem., 63, 837 (1959).

[3] CHARLESBY, A., *Atomic Radiation and Polymers*, Pergamon Press, New York (1960).

[4] CHAPIRO, A., *Radiation Chemistry of Polymeric Systems*, Interscience Publishers, New York (1962).

[5] CUNLIFFE, A. V. and DAVIS, A., Polym. Degrad, Stab., 4, 17 (1982).

[6] GILLEN, K.T. and CLOUGH, R.L., in Handbook of Polymer Science and Technology, Vol. 2: Performance Properties of Plastics and Elastomers, Ch. 6, N. P. Cheremisinoff, Ed., Marcell Dekker, Inc., New York (1989).

[7] GILLEN, K.T. and CLOUGH, R.L., in Irradiation Effects on Polymers, Ch. 4, CLEGG, D.W. and COLLYER, A. A., Eds., Elsevier Applied Science Publishers Ltd., London (1991).

[8] SEGUCHI, T., HASHIMOTO, S., KAWAKAMI, W. and KURIYAMA, E., Radiation Damage of Polymer Materials. I. Simulation Studies on Distribution of Oxygen Concentration in Polymer Film under Irradiation in Oxygen, Japan Atomic Energy Research Institute Report, JAERI-M 7315 (1977).

[9] [9] SEGUCHI, T. and YAMAMOTO, Y., *Diffusion and Solubility of Oxygen in Gamma-Ray Irradiated Polymer Insulation Materials*, Japan Atomic Energy Research Institute Report, JAERI-M 1299 (1986).

[10] CLOUGH, R. L. and GILLEN, K.T., Polym. Deg. and Stabil., 38, 47 (1992).

[11] CLOUGH, R. L. and GILLEN, K.T. and QUINTANA, C.A., J. Polym. Sci., Polym. Chem. Ed., 23, 359 (1985).

[12] CLOUGH, R.L. and GILLEN, K.T., in Polymer Stabilization and Degradation, ACS Symposium Series No. 280, p. 411, P. P. Klemchuk, Ed., American Chemical Society, Washington, D.C. (1984).

[13] GILLEN, K.T., CLOUGH, R. L. and and DHOOGE, N.J., Polymer, 27, 225 (1986).

[14] GILLEN, K.T., CLOUGH, R. L. and QUINTANA, C.A., Polym. Degrad. and Stab., 17, 31 (1987)

[15] GILLEN, K.T. and CLOUGH, R.L., Polym. Eng. and Sci., 29, 29 (1989).

[16] SEGUCHI, T., HASHIMOTO, S., ARAKAWA, K. HAYAKAWA, N., KAWAKAMI, W. and KURIYAMA, I., Radiat. Phys. Chem., 17, 195 (1981).

[17] GIBERSON, R.C., J. Phys. Chem. 66, 463 (1962).

[18] MOISAN, J. Y., in *Polymer Permeability*, p. 119, J. Comyn, Ed., Elsevier Applied Science Publishers, London (1985).

[19] PAPET, G., AUDOUIN-JIRACKOVA, L. and VERDU, J., Radiat. Phys. Chem., 33, 329 (1989).

[20] JOUAN, X. and GARDETTE, J.L., Polym. Commun., 28, 329 (1987).

[21] JOUAN, X., ADAM, C., FROMAGEOT, D., GARDETTE, J.L. and LEMAIRE, J., Polym. Degrad. and Stabil., 25, 247 (1989).

[22] GILLEN, K.T. and CLOUGH, R.L., Polym. Preprints, 31, No. 2, 387 (1990).

[23] GILLEN, K.T. and CLOUGH, R.L. in *Radiation Effects on Polymers*, R. L. Clough and S. Shalaby, Eds., ACS Symposium Series, No. 475, American Chemical Society, Washington, D.C. (1991), p. 457.

[24] MORITA, Y., YAGI, T. and KAWAKAMI, W. in *Radiation Effects on Polymers*, R. L. Clough and S. Shalaby, Eds., ACS Symposium Series, No 457, American Chemical Society, Washington, D.C. (1991), p. 485.

[25] BOWMER, T.N., COHEN, L.K., O'DONNELL, J.H. and WINZOR, D.J., *J. Appl. Polym. Sci.*, 24, 425 (1979).

[26] BELOUSOVA, M.V., SKIRDA, V.D., ZGADZAI, O.E., MAKLALOV, A.I., POTAPOVA, I.V., ROMANOV, B.S. and RUMYANTHEV, D.D., *Acta Polym.*, 36, 557 (1985).

[27] WILSKI, H., GAUBE, E. and ROSINGER, S., *Kerntechnik*, 5, 281 (1963).

[28] WILSKI, H., Kunstoffe, 53, 862 (1963).

[29] KURIYAMA, I., HAYAKAWA, N., NAKASE, Y., OGURA, J., YAGYU, H. and KASAI, K., IEEE Trans. Electr. Insul., EI-14, 272 (1979).

[30] YOSHII, F., SASAKI, T., MAKUUCHI, K. and TAMURA, N., *J. Appl. Polym. Sci.*, 31, 1343 (1986)

[31] BILLINGHAM, N.C. and CALVERT, P.D., in *Developments in Polymer Stabilisation*, Vol. 3, G. Scott, Ed., Applied Science Publishers, Ltd. (1980).

[32] *Polymer Permeability*, J. Comyn, Ed., Elsevier Applied Science, London (1985).

[33] *Engineering Design for Plastics*, E. Baer, Ed., Reinhold Publ. Corp., New York (1964).

[34] FELDER, R.M. and HUVARD, G.S., in *Methods of Experimental Physics*, 16c, pp. 315-377, Academic Press, New York (1980).

[35] STANNETT, V.T., *Polym. Eng. Sci.*, 18, 1129 (1978).

[36] HWANG, S.T., CHOI, C.S. and KAMMERMEYER, K., *Separ. Sci.*, 9, 461 (1974).

[37] PAULY, S. in *Polymer Handbook*, 3rd Ed., pp. VI/435-449, J. Brandrup, and E.H. Immergut, E.H., Eds., John Wiley and Sons, New York (1989).

[38] ARAKAWA, K., SEGUCHI, T., WATANABE, Y., HAYAKAWA, N., *J. Polym. Sci., Polym. Chem.* Ed., 20, 2681 (1982).

[39] ARAKAWA, K., SEGUCHI, T., HAYAKAWA, N., MACHI, S., *J. Polym. Sci., Polym. Chem*. Ed., 21, 1173 (1983).

[40] ARAKAWA, k., SEGUCHI, T., WATANABE, Y., HAYAKAWA, N., KURIYAMA, I., MACHI, S., *J. Polym. Sci., Polym. Chem*. Ed., 29, 2123 (1981).

[41] ARAKAWA, K., SEGUCHI, T. and YOSHIDA, K., *Radiat. Phys. Chem.*, 27, 157 (1986).

[42] SEGUCHI, T., YAMAMOTO, Y. and YAGYU, H., Hitachi Cable Review, 4, 37 (1985).

[43] SEGUCHI, T., ITO, H. and YOSHIDA, K., Design and Construction of Accelerated Ageing Facility for Cables, Japan Atomic Energy Research Institute Report, JAERI-M 83-089 (1983).

[44] BOLLAND, J.L., Proc. Roy. Soc., 186, 218 (1946).

[45] BATEMAN, L., Quarterly Rev. (London), 8, 147 (1954).

[46] KUDO, H. and TEZUKA, S., to be published.

[47] CRANK, J. “The mathematics of diffusion”, Clarendon Press, Oxford, England, 1975.

———————

This page deliberately left blank

This page deliberately left blank

British Standards Institution (BSI)

BSI is the national body responsible for preparing British Standards and other standards-related publications, information and services.

BSI is incorporated by Royal Charter. British Standards and other standardization products are published by BSI Standards Limited.

About us

We bring together business, industry, government, consumers, innovators and others to shape their combined experience and expertise into standards -based solutions.

The knowledge embodied in our standards has been carefully assembled in a dependable format and refined through our open consultation process. Organizations of all sizes and across all sectors choose standards to help them achieve their goals.

Information on standards

We can provide you with the knowledge that your organization needs to succeed. Find out more about British Standards by visiting our website at bsigroup.com/standards or contacting our Customer Services team or Knowledge Centre.

Buying standards

You can buy and download PDF versions of BSI publications, including British and adopted European and international standards, through our website at bsigroup.com/shop, where hard copies can also be purchased.

If you need international and foreign standards from other Standards Development Organizations, hard copies can be ordered from our Customer Services team.

Subscriptions

Our range of subscription services are designed to make using standards easier for you. For further information on our subscription products go to bsigroup.com/subscriptions.

With **British Standards Online (BSOL)** you'll have instant access to over 55,000 British and adopted European and international standards from your desktop. It's available 24/7 and is refreshed daily so you'll always be up to date.

You can keep in touch with standards developments and receive substantial discounts on the purchase price of standards, both in single copy and subscription format, by becoming a **BSI Subscribing Member**.

PLUS is an updating service exclusive to BSI Subscribing Members. You will automatically receive the latest hard copy of your standards when they're revised or replaced.

To find out more about becoming a BSI Subscribing Member and the benefits of membership, please visit bsigroup.com/shop.

With a **Multi-User Network Licence (MUNL)** you are able to host standards publications on your intranet. Licences can cover as few or as many users as you wish. With updates supplied as soon as they're available, you can be sure your documentation is current. For further information, email bsmusales@bsigroup.com.

BSI Group Headquarters

389 Chiswick High Road London W4 4AL UK

Revisions

Our British Standards and other publications are updated by amendment or revision.

We continually improve the quality of our products and services to benefit your business. If you find an inaccuracy or ambiguity within a British Standard or other BSI publication please inform the Knowledge Centre.

Copyright

Useful Contacts:

Customer Services
Tel: +44 845 086 9001
Email (orders): orders@bsigroup.com
Email (enquiries): cservices@bsigroup.com

Subscriptions
Tel: +44 845 086 9001
Email: subscriptions@bsigroup.com

Knowledge Centre
Tel: +44 20 8996 7004
Email: knowledgecentre@bsigroup.com

Copyright & Licensing
Tel: +44 20 8996 7070
Email: copyright@bsigroup.com

bsi.

...making excellence a habit.™